20S Proteasome and Its Inhibitors: Crystallographic Knowledge for Drug Development

Ljudmila Borissenko and Michael Groll*

Charité (CCM), Institut für Biochemie, AG Strukturforschung, Monbijoustrasse 2, 10117 Berlin, Germany

Received May 23, 2006

Contents

* To whom correspondence should be addressed. Telephone: +49-(0)30-450-528304. Fax: +49-(0)30-450-528903. E-mail: michael.groll@charite.de.

1. Introduction

Principles of intracellular protein synthesis and protein degradation remain to be among the most challenging questions of modern cell biology. Proteolysis plays an important role in maintaining biological homeostasis and regulation of different intracellular processes. The major component of the nonlysosomal protein degradation pathway is the proteasome, which is found in eukaryotes as well as in prokaryotes. Proteasomes are involved in a variety of essential biological processes: protein quality control, antigen processing, signal transduction, cell cycle control, cell differentiation, and apoptosis. Crystal structures of the prokaryotic and eukaryotic core proteasomal complexes provided valuable information on the composition, assembly, catalytic mechanism, and regulation of this major proteolytic machinery of the cell. In sections 2 and 3 of this review, we discuss state of the art conceptions of the cellular protein degradation processes, focusing on the structural organization, assembly, and proteolytic mechanism of the core proteasome complex from both pro- and eukaryotes.

Insights provided by elucidation of proteasomal activity mechanisms opened broad perspectives for inhibition and regulation of proteasomes by various chemical compounds. Section 4 is dedicated to a detailed description of the major classes of proteasomal inhibitors. Some of the chemical compounds which are able to efficiently and selectively inhibit proteasomal activity have already found their application in biology and medicine as a means to investigate the proteasome and its cellular role and eventually to create a basis for treatment of many life threatening diseases, which is briefly discussed in section 5.

Overall, the major aim of this review is to make the reader familiar with the latest insights on the structure and function

10.1021/cr0502504 CCC: $65.00
Published on Web 02/23/2007

Ljudmila Borissenko received her Master of Science Degree in Biology at the Saint-Petersburg State University. She completed her Ph.D. at the Georg-August-University in Göttingen, where she studied the genetic and molecular basis of multiple sulfatase deficiency, a lethal lysosomal storage disease. Afterward, she moved to the Ludwig-Maximilians-University in Munich and joined the lab of Prof. Walter Neupert as a postdoctoral fellow, concentrating on structural and functional studies of components of cellular protein degradation systems as well as membrane translocation machineries. Currently, she is working as a senior researcher at the Charité Medical School of the Humboldt-University in Berlin.

Michael Groll studied chemistry at the Technical University of Munich and then joined the laboratory of Prof. Robert Huber for postgraduate studies. In 1998, he received his Ph.D. for crystallographic and biochemical studies on the 20S proteasome from *S. cerevisiae*. In 2002 he joined the group of Prof. Daniel Finley at Harvard Medical School as a guest researcher, being involved in the elucidation of structural and functional mechanisms of proteasomal regulation. From 2003 to 2007, he was running an independent research group at the Adolf Butenandt-Institute of Physiological Chemistry at the Ludwig-Maximilians-University in Munich. In 2004, he completed his Habilitation at the Charité in Berlin for his work on structural and functional relationships between archaebacterial and eukaryotic 20S proteasomes. In 2006, he accepted an appointment as a professor for biochemistry at the Charité Medical School of the Humboldt-University in Berlin. His current main research interests are focused on functional and structural characterization of multifunctional protein complexes; structural characterization of protein–protein and protein–ligand interactions; development and practical application of synthetic and natural protein ligands; as well as molecular flexibility and its biological significance.

of the proteasome, highlighting the structural features that determine its activity and specificity. The main focus has been on the current structural knowledge of the mechanisms of regulation and modulation of proteasomal activity by various natural and synthetic chemical compounds, showing the proteasome as a potential target for drug development in biomedical research. This review describes in detail the mechanisms of action of various proteasomal inhibitors and

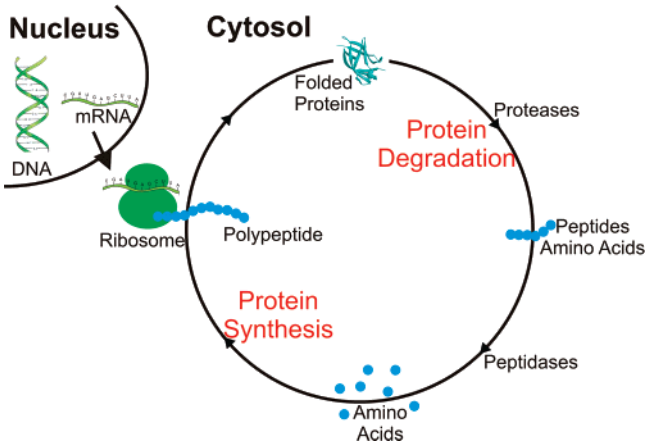

Figure 1. Life cycle of proteins.

spans scientific publications mainly of the period from 1997 to 2006.

2. Nonlysosomal Protein Degradation

Protein synthesis and protein degradation are two universal complementary processes, permanently occurring in a living cell (Figure 1). ATP-dependent proteolysis, first identified in crude extracts of reticulocytes,[1] plays an important role in maintaining biological homeostasis and regulation of different cellular processes, such as cell differentiation, cell cycle control, antigen processing, and hormone metabolism. In eukaryotes, the nonlysosomal protein degradation is performed by the strictly controlled complex enzymatic machinery of the ubiquitin−proteasome pathway. This pathway plays a primary role in the degradation of the bulk of proteins in mammalian cells, as well as the degradation of abnormal proteins, and thus produces most of the antigenic peptides presented to the immune system by MHC (Major Histocompatibility Complex) class I molecules. The proteasome is involved in the turnover of many critical proteins involved in the control of cell growth, cell differentiation, or metabolic adaptation.

The degradation of folded proteins to single amino acids is a strictly controlled and multistep process. In order to be recognized by the proteolytic system and targeted for degradation, eukaryotic proteins are marked by covalent addition of ubiquitin chains,[2,3] which serve as a recognition signal for the 19S regulatory particle and interacting proteins.[4] The poly-ubiquitination reaction requires the action of several enzymes, which function sequentially to covalently attach ubiquitin to a lysine residue of a substrate or of the previous ubiquitin molecule in the chain.[5] The action of the ubiquitinating enzymes is countered by that of de-ubiquitinating enzymes, or isopeptidases, which are able to remove ubiquitin from poly-ubiquitinated substrates. De-ubiquitination might be important in reversing the ubiquitination of specific proteins and, thus, in preventing, possibly transiently, their degradation.[6] The understanding of targeting and recognition of protein substrates in prokaryotes is still incomplete. Bacteria and mitochondria lack ubiquitin, and it has been postulated that they do not have any similar substrate-marking system. However, recently it was found that, in *E. coli*, proteins are marked for degradation by addition of a C-terminal marker peptide of 11 amino acids, named SsrA,[7,8] which is considered to be a bacterial analogue of ubiquitin.

Once ubiquitinated, the proteins are rapidly degraded to small peptides by the 26S proteasome complex, the main proteolytic component of the ubiquitin−proteasome degradation pathway, which is found in all eukaryotic cells.[9,10] The marked substrates are recognized by the proteasomal 19S complex (regulatory particle), which performs various functions, including recognition and binding of polyubiquitin chains,[11] release of free ubiquitin,[12] and ATPase function[13] as well as protein unfoldase function. The proteins are being unfolded and translocated into the lumen of the 20S proteasome, which carries the proteolytically active sites, where they are degraded into short peptides. In addition to the 19S complex, the 20S proteasome can separately interact with other regulatory complexes such as PA28[14] or PA200.[15] Both complexes are able to activate the proteolytic activity of the 20S proteasome upon binding to its poles. Interestingly, hybrid molecules made of one 20S proteasome bound to one 19S complex and one PA28 have been found in cell extracts,[16] though the physiological role of these complexes is still under debate.

In both pro- and eukaryotes, proteasomes are the major but not the only protein degradation machinery: there exist alternative protein degradation pathways, represented by Lon protease, found in bacteria, *archaea*, and mitochondria,[17,18] FtsH protease from bacteria and *archaea*,[19,20] as well as ClpAP, ClpXP, and HslUV proteolytic complexes from bacteria.[21−23] These systems exhibit redundant proteolytic activities, despite differences in their overall structural architecture and catalytic properties.[24,25] It is remarkable that, despite their abundance, all these proteolytic machines are not able to complete the degradation process and to cleave proteins to single amino acids. They all generate a pool of oligopeptides of different length, some of which are presented on the cell surface for generation of immune response, but the majority of these peptides are being further processed by different cytosolic peptidases.

Tricorn protease (TRI), a 720 kDa hexameric complex discovered in *Thermoplasma acidophilum*, was the first identified protease, which performs degradation of oligopeptides produced by the proteasome.[26] It is able to digest oligomeric peptides to tri- and dipeptides,[27,28] which are degraded sequentially to free amino acids by peptidases named tricorn interacting factors F1, F2, and F3.[29−31] TRI is only present in the genomes of some prokaryotes, and primary sequence alignment reveals no homologues in eukaryotes. TPPII, a giant protease complex identified in mammalian cells possesses exoproteolytic and endoproteolytic activities, and is believed to function as the eukaryotic homologue of TRI, processing oligopeptides produced by proteasomes.[32−34] Recently, there was discovered a novel prokaryotic protease complex, named TET protease,[35] which exhibits broad aminopeptidase activity and which is able to degrade peptides produced by the proteasome to single amino acids.[36,37] Interestingly, among prokaryotes, the genomic distribution of TRI and TET proteases is not overlapping. All these proteolytic enzymes are essential for complete degradation of the protein from the folded state up to free amino acids, which can be further used in cell metabolism.[36]

Regulated degradation of specific proteins is necessary for a large range of cellular processes important, in particular, for cell integrity, proliferation, and differentiation. Dysfunction of the degradation machinery can lead to aberrant expression of proteins and consequent deleterious effects for the cell or the organism.[38] Consequently, there exists considerable interest in manipulation of the ubiquitin−proteasome system in order to control the stability of important regulatory proteins. The proteasome remains the main potential target for regulation of proteolysis, in particular for treatments of pathologies associated with excessive degradation of one or more proteins.[39] There is a large effort, reflected by the increasing number of reports, to develop and study new molecules able to block the activity of the proteasome and, thus, to manipulate various cellular processes. Modern structural methods, such as electron microscopy, NMR, and X-ray crystallography, are used to elucidate the three-dimensional structures of proteasomal inhibitor molecules bound to the active sites. Structural data obtained with these methods have proved to be valuable in providing essential information and insights for further improvement of existing inhibitors and structure-based design of the new compounds.

3. Structure and Mechanism of Action of the Proteasome

3.1. The 26S and 20S Proteasome

The 26S proteasome complex is a multifunctional, 2,500,000 Da proteolytic molecular machine, in which several enzymatic (proteolytic, ATPase, de-ubiquitinating) activities function together with the ultimate goal of protein degradation.[40] In eukaryotes, 26S proteasomes are composed of the cylinder-shaped multimeric protein complex referred to as the 20S proteasome core particle, capped at each end by the regulatory component termed the 19S complex (regulatory particle or PA700).[41,42] The substrates are processed at the active sites located within the inner cavity of the 20S proteasome, whereas the 19S regulatory particle is responsible for recognition, unfolding, and translocation of the selected substrates into the lumen of the 20S proteasome.[10]

The 20S proteasome is a large, cylinder-shaped protease with a molecular weight of about 700,000 Da. It plays the crucial role in cellular protein turnover and is found in all three kingdoms of life. Electron micrographs of 20S proteasomes revealed its molecular dimensions to be ∼160 Å in length and ∼120 Å in diameter.[43] The complex is formed by 28 protein subunits, which are arranged in four stacked rings, each comprising seven subunits.[44] The detailed composition of subunits was first elucidated by crystal structure analysis of the archaebacterial proteasome from *Thermoplasma acidophilum* at 3.4 Å resolution.[45] Since then, the crystal structures have been elucidated for 20S proteasomes from the following procaryotes: *Archaeoglobus fulgidus*,[46] *Rhodococcus erythropolis*,[47] and *Mycobacterium tuberculosis*.[138] The structural data showed that all prokaryotic 20S proteasomes have the shape of an elongated cylinder with three large cavities and narrow constrictions between them. The proteasomal complex has 72 point symmetry following an $\alpha_7\beta_7\beta_7\alpha_7$-stoichiometry. The two outer chambers are formed by α- and β-rings, whereas the central chamber, containing the proteolytic active sites, is composed of the β-rings. Though the primary sequences of α- and β-subunits are quite different, they show similar folding, which is also found in the subunits of HslV,[48,49] the proteasomal analogue of eubacteria (Figure 2). This common folding pattern may indicate that these proteases originate from an ancestral gene, which already existed before the evolutional divergence of the three kingdoms of life. The fold of the subunits is characterized by a sandwich of two five-stranded antiparallel

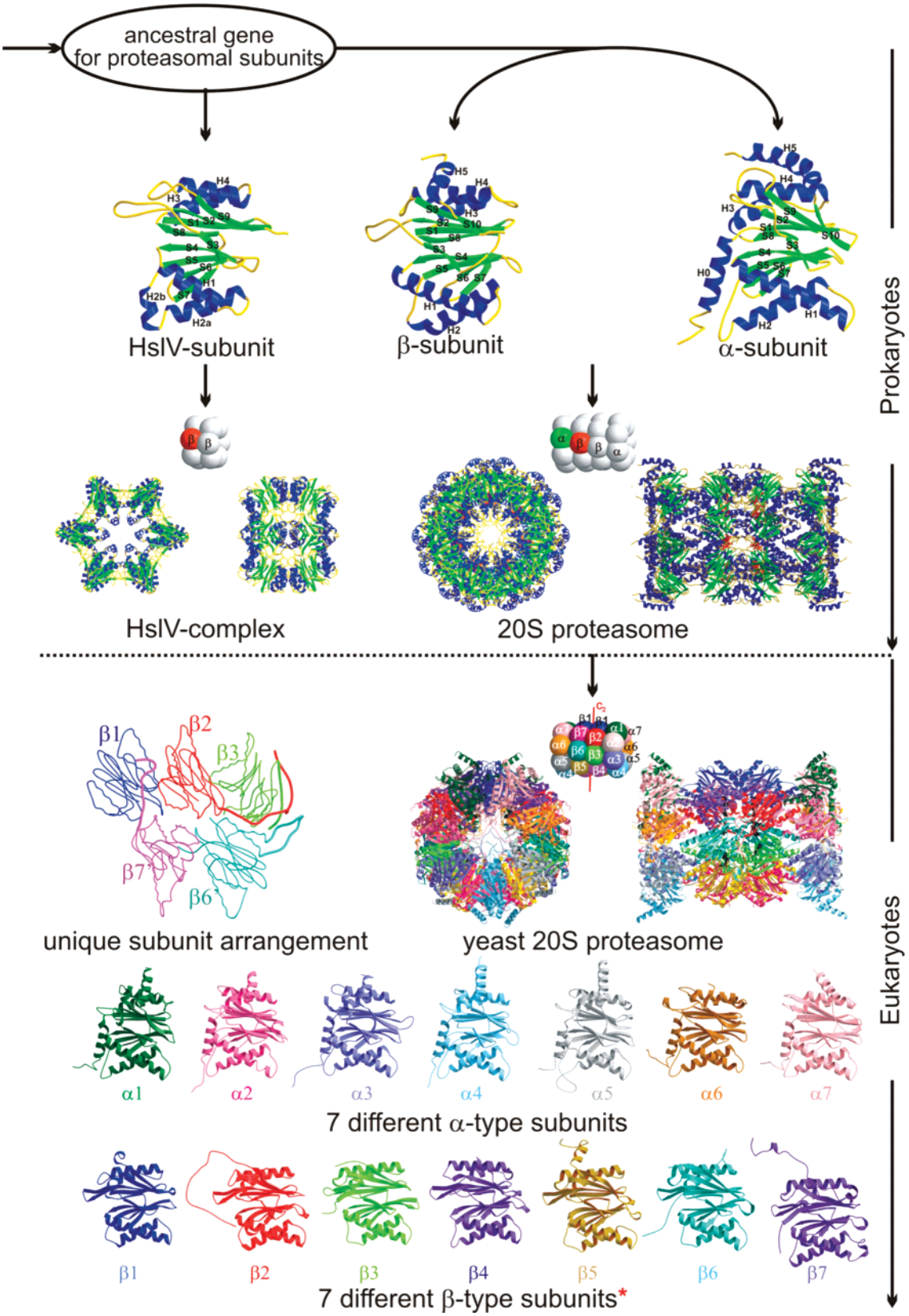

Figure 2. Development of proteasomes and proteasome-like complexes in archaebacteria, eubacteria and eukaryotes.[45,47,49−51]

β-sheets, which are flanked by helical layers on the top and the bottom. Archaebacterial proteasomes can be regarded as the prototype for the quaternary structure and topology of proteasomes, whereas the general architecture of eukaryotic proteasomes is much more complex.[50,51] Crystal structures of yeast[50,52] and bovine[51] proteasomes showed that, in eukaryotes, α- and β-subunits have each diverged into seven different subunits (Figure 3). Eukaryotic proteasomes show pseudo-sevenfold symmetry and consist of two equal parts ($\alpha_{1-7}\beta_{1-7}\beta_{1-7}\alpha_{1-7}$), which are related by twofold symmetry. The nomenclature of each subunit is defined according to the structural data from the yeast proteasome.[50] All 14

Figure 3. Sequence alignment of the various proteasomal β-type subunits from *T. acidophilum*, yeast, and human. Prosegments of proteolytically active subunits are removed; subunits β3, β6, and β7 are shown with their partially processed precursor sequence. Helices and β-strands are shown as black cylinders and arrows, respectively. Residues involved in the formation of the catalytic active sites are marked in red. Proteolytically active subunits β1, β2, and β5 are additionally aligned with their related interferon-inducible γ-subunits. Residues which form the bottom of the nonprimed S1 specificity pocket are shown in blue. So far, residues contributing to the primed substrate binding channel have been elucidated only for subunit β5 (highlighted in green). Note the differences between constitutive and γ-interferon inducible subunits in the S1 specificity pocket of subunit β1 and in the primed substrate binding channel of subunit β5.[45,50,94]

different eukaryotic proteasomal subunits contain characteristic insertion segments and termini (Figure 2), which represent well-defined contact sites between related subunits and cause their unique locations at special positions within the particle. Compared to archaebacterial proteasomes, which have 14 identical and thus 14 proteolytically active sites, eukaryotic proteasomes contain only three proteolytically active β-type subunits per β-ring (subunits β1, β2, and β5), whereas the other β-type subunits are inactive. In mammalian proteasomes, γ-interferon provokes the substitution of these three active β-subunits (β1, β2, and β5) for three newly synthesized LMP subunits termed β1i, β2i, and β5i (Figure 4e).[53−57] The incorporation of the γ-interferon inducible subunits into the proteasome requires its *de novo* assembly and depends on the cell development state and the tissue type.[58,59] These γ-interferon inducible subunits are referred

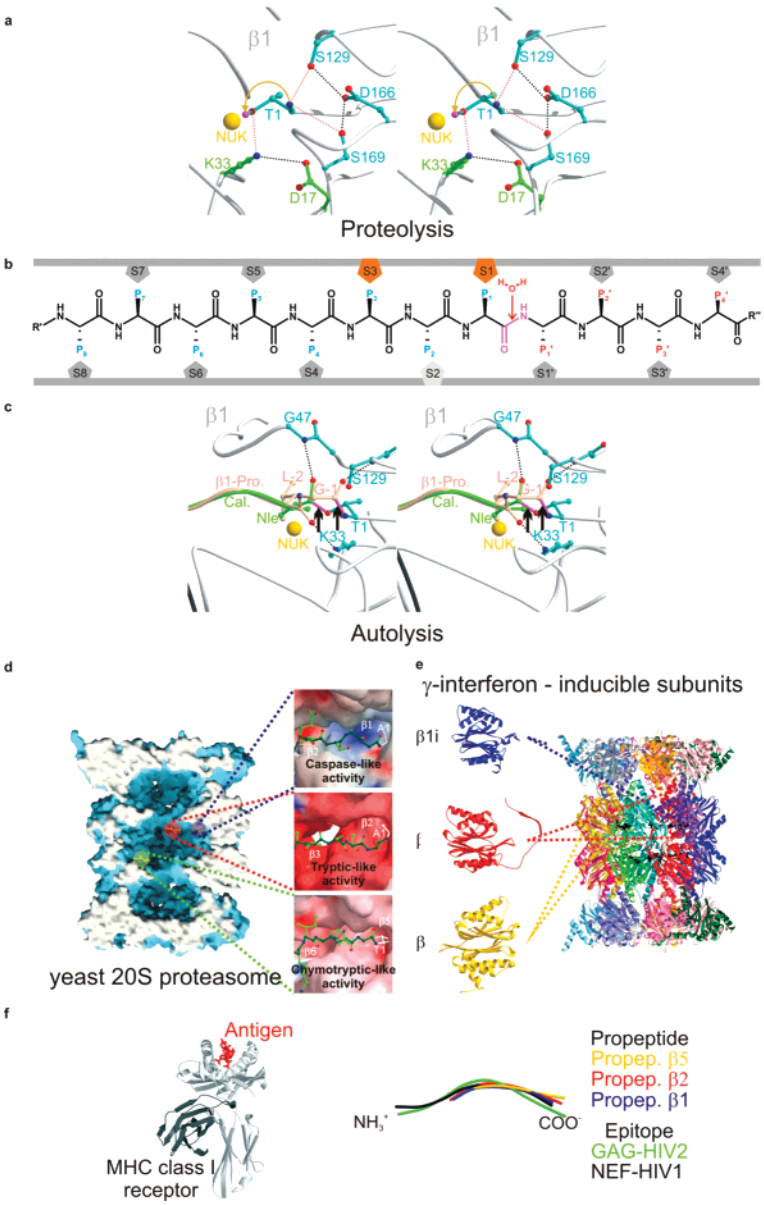

Figure 4. Architecture and active site mechanism. Stereorepresentation of proteolysis and autolysis in proteasomes. (a) The surroundings of the catalytic residue Thr1 in subunit β1. The protein backbone is drawn as white coils, whereas residues which form the active site (Thr1, Asp17, Lys33, Ser129, Asp166, and Ser169) are shown as balls-and-sticks. Lys33 forms a salt bridge with Asp17 (purple dashed lines; both residues are colored in green) and therefore is presumably positively charged, lowering the pK_a of the Thr1O$^{\gamma}$ electrostatic potential (black dashed lines). Close to Thr1 are residues Ser129, Asp166, and Ser169 (colored in blue), which are required for the conformational stability of Thr1 (purple dots). A cluster of solvent molecules, NUK (shown as yellow spheres) is localized in the electron density close to Thr1O$^{\gamma}$ and N and presumably plays a major role in the proton transfer (yellow circle).[45,50,63] (b) Standard orientation for peptides bound to the proteasomal specificity pockets. The substrate is oriented from its N- to its C-terminus. The scissile peptide bond is shown in magenta, flanked by the nucleophilic water molecule which is incorporated into the product during hydrolysis. Residues on the left site of the scissile peptide bond, which generate the C-terminal part of the product, are termed nonprimed P sites; residues on the right site are termed primed P′ sites. Specificity pockets, which are responsible for ligand stabilization, are termed S and S′ pockets, respectively.[81,251] (c) Proposed mechanism for autolysis and substrate proteolysis shown at the example of the active site of the yeast 20S proteasome subunit β1 (backbone shown as white coils and Thr1 as blue balls-and-sticks). Calpain inhibitor I and the β1-propeptide are green and pink, respectively. Proteolysis and autolysis (black arrows) are initiated by proton transfer from Thr1O$^{\gamma}$ to NUK (shown as yellow sphere). Gly47N is the major constituent of the oxyanion-hole for inhibitors and substrates, lowering the energy of the tetrahedral adduct transition state.[50] Ser129N is the essential part of the oxyanion-hole for the carbonyl oxygen of Gly-1, whereas Lys33N$^{\zeta}$ stabilizes the carbonyl oxygen of position −2 in the propeptides.[69] Hydrogen bonds are indicated as black dashed lines. Addition of Thr1O$^{\gamma}$ to the carbonyl carbon of Gly-1 (autolysis) or to norleucine (proteolysis) is followed by ester bond formation, which is hydrolyzed in both pathways by incorporation of the nucleophilic water molecule into the product. (d) Surface representation of the yeast 20S proteasome in complex with propeptides, clipped along the cylindrical pseudo-sevenfold symmetry axis. Propeptides are shown as space-filling models in yellow and illustrate the nonprimed substrate binding channel of the proteolytically distinct active sites.[63] The various proteolytic active centers are marked in a specific color coding: subunit β1 in blue; subunit β2 in red; subunit β5 in green. Caspase-, tryptic-, and chymotryptic-like active sites are enlarged and illustrated as surfaces; propeptides are presented as ball-and-stick models.[114] Surface colors indicate positive and negative electrostatic potential contoured from 15kT/e (intense blue) to −15kT/e (intense red). (e) Topology of the 28 subunits of the yeast 20S proteasome in ribbon presentation. γ-Interferon inducible mammalian subunits β1i, β2i, and β5i are modeled by the corresponding constitutive yeast subunits.[50,51] (f) MHC class I molecule in complex with an antigen (left panel).[252] Structural superposition of propetides β1, β2, and β5 with NEF-HIV1 and GAG-HIV2 antigen bound to MHC class I molecules (right panel).[94]

to as the immuno subunits, as they tune the 20S proteasome for higher efficiency to generate specific antigenic peptides.[60,61] These peptides are finally loaded on MHC class I proteins and eventually participate in the initiation of the immune response (Figure 4f).

3.2. Proteolysis versus Autolysis in Proteasomes

The activity of the 20S proteasome was shown to be sensitive to different types of protease inhibitors, but the true proteolytic nature of the active sites within this complex remained obscure for several years. Eventually, the crystal structure of the proteasome from *T. acidophilum* in complex with the competitive inhibitor Ac-Leu−Leu-nLeu-al (calpain inhibitor I) showed for the first time that the proteolytic active centers in archaebacterial proteasomes are formed by the N-terminal threonine of each of the β-subunits.[45] The functional aldehyde group of the inhibitor was shown to be covalently bound to the Thr1O$^{\gamma}$ by formation of a hemiacetal bond.

Proteasomes are not the only proteins which use the N-terminal threonine as a catalytic residue. The topology of proteasomal subunits was found to be characteristic for a set of hydrolases that show no recognizable sequence similarity to each other. This class of proteins use their N-terminal residue as the nucleophile and, therefore, were named N-terminal nucleophilic (Ntn) hydrolases.[62] Currently, there are already 20 documented crystal structures of Ntn hydrolases deposited in the RCSB protein data bank. Surprisingly, the active site residues of this class of proteins are not conserved, supporting the assignment of the common N-terminal amino group as the proton acceptor in proteolysis.[63,67] All Ntn hydrolases require a processing step which results in the exposure of the N-terminal nucleophilic amino group. Consequently, proteasomes have to follow a defined maturation pathway leading to creation of the functionally active Ntn−protease complex. During the consecutive maturation process, the prosegments of the β-subunit precursor complexes are removed by intramolecular autolysis, resulting in the proteolytically active protease complex.[46,64,65] In experiments with yeast proteasome, where the propeptide of subunit β1 was replaced by ubiquitin, which liberated the N-terminal threonine immediately after expression, the subunit remained inactive.[66,67] Structural analysis of the mutant proteasome showed no significant differences from the wild type structure, with the exception of extra electron density at the amino group of Thr1 of subunit β1, which was interpreted as an acetyl group and confirmed by mass spectroscopy.[63] The acetyl group is not cleaved by autolysis, probably for sterical reasons. In parallel, mutagenesis experiments with yeast proteasome could show that all proteolytically active subunits are activated after deletion of their respective propeptides when the Nα-acetyltransferase is inactivated.[67] These observations support the proteolytic mechanism assigning the role of the proton acceptor to the amino group of Thr1 (Figure 4a).

Structural and mutational studies on the prokaryotic proteasome could define Thr1, Glu17, and Lys33 as the major important residues involved in the proteolytic mechanism. Additionally, Ser129, Asp166, and Ser169, which are close to the active site Thr1, seem to be required for the structural integrity of the proteolytic center as well as being involved in catalysis (Figure 4a).[45,68] The crystal structures of the yeast and bovine liver proteasomes,[50,51] as well as the characterization of various mutants,[63,69] could finally elucidate the proteolytic mechanism at the proteasomal active sites. These reports demonstrate that Thr1O$^{\gamma}$ reacts with electrophilic functional groups of inhibitors or peptide bonds of substrates, while Thr1N represents the proton acceptor. The N-terminus of the nucleophilic threonine is hydrogen bridged to Ser129O$^{\gamma}$, Asp166O, and Ser169O$^{\gamma}$, whereas the Thr1O$^{\gamma}$ is hydrogen bonded to Lys33N$^{\zeta}$ (Figure 4a). The pK_a and status of protonation of the ionizable groups is unknown, but the pattern of hydrogen bonds suggests that at least Lys33N$^{\zeta}$ is charged. Indeed, in yeast, the substitution of conserved active Lys33 with Arg33 in subunit β5 leads to its inactivation.[63] The structural superposition of this mutant with the wild type shows some sterical rearrangements at the active site: Arg33 has its guanidino group tilted compared to the amino group of the lysine residue to avoid a clash with Thr1. This rearrangement is possibly associated with effects on the intrinsic pK_a of Thr1O$^{\gamma}$ and Th1N, thus preventing the hydrolysis of substrates. Besides the N-terminal threonine, a cluster of water molecules (termed NUK), usually located in proximity to Thr1O$^{\gamma}$, Thr1N, Ser129O$^{\gamma}$, and Gly47N, also plays a key role in proteolysis (Figure 4c).[50,70] It has been absent in the electron density map of the proteasome from *T. acidophilum* at lower resolution but was seen in the structures of the yeast proteasome and penicillin acylase,[71] another member of the Ntn-hydrolase family. The possible function of the water molecule is to serve as the proton shuttle between Thr1O$^{\gamma}$ and Thr1N during substrate binding and to participate in the cleavage of the acyl ester intermediate with the resulting regeneration of Thr1O$^{\gamma}$[50,70] (Figure 4c).

During proteasomal maturation, prosegments of inactive β-subunits are removed by autolysis between residues Gly-1 and Thr1, a process requiring a Gly-Thr site and catalytic residues. Mutants of eukaryotic proteasomes[58,72,73] and naturally occurring inactive proteasomal subunits altered at those sites are not processed. As has been shown for the yeast β1Thr1Ala proteasome mutant, the conformation of the segment Leu-2 to Thr1 has a bulge at Gly-1 with a short hydrogen bond (2.5 Å) between Leu-2O and Thr1N, classified as a three-residue γ-turn. γ-Turns show no significant sequence preference, and the conservation of Gly-1 in proteasomes may serve to avoid sterical interference of side chains with the turn segment at position 168. Thr1O$^{\gamma}$ is centrally positioned among the γ-turn and in proximity to the carbonyl carbon atom of Gly-1, so that further approach by a Thr1 side chain rotation and pyramidalization of the carbonyl carbon atoms follow the preferred trajectory of a nucleophilic addition reaction.[74] In contrast to the case of proteolysis, the N-terminal amino group is engaged in the autolysis reaction and, therefore, is not available as a proton acceptor. The nucleophilic water molecule (NUK) is ideally positioned to act as the general base and promote the abstraction of the proton from the Thr1 hydroxyl group, initiating nucleophilic attack of the Thr1O$^{\gamma}$ on the carbonyl carbon of the preceding Gly-1 peptide bond (Figure 4c).[69] The following addition leads to a hydroxazolidine intermediate, which may decay to the ester, when the C−N-bond is cleaved. The nucleophilic water molecule functions as the base in the addition reaction and, after a slight rearrangement, as proton donor to the amido nitrogen, when the C−N-bond is cleaved and the ester bond is formed. The water molecule may finally be incorporated into the product when the ester is hydrolyzed during active site regeneration. Thus, the proteasomal active sites are designed for both reactions:

intramolecular autolysis and substrate proteolysis. Subunits β3, β4, and β6 lack the nucleophilic threonine in position 1 and, thus, are inactive. So far, attempts at reactivation of inactive β-type subunits by multiple mutations failed,[63] whereas inactivation of active subunits is possible but causes severe phenotypes.[72,75]

Although subunit β7 has conserved Thr1 and Gly-1 residues similar to proteolytically active proteasomal subunits, this subunit remains inactive as well. Crystallographic analysis of yeast and bovine 20S proteasomes showed that the propeptide of subunit β7 is not autolyzed at Thr-1 but is cleaved at position Thr-8 during the maturation process. The autolytic reaction cannot take place at Thr-1 due to evolutional substitutions of proteolytically and autolytically essential residues such as Lys33 and Ser129 to Arg33 and Phe129, respectively. On the basis of the crystal structure of the bovine 20S proteasome, it was proposed that subunit β7 possesses Ntn hydrolase proteolytic activity[51] at Thr-8. However, the surroundings of the proposed active site differ significantly from those of subunits β1, β2, and β5, and therefore, these data need experimental confirmation, such as active site kinetics or binding of inhibitors to subunit β7.

3.3. Degradation of Unfolded Proteins and Generation of Oligopeptides

The lengths of the cleavage products produced by proteasomes vary between 3 and 25 amino acids with an average length distribution of 8 to 12 amino acids. Until recently, the mechanism of peptide product length control was unclear. The crystal structure of the 20S proteasome from *T. acidophilum* revealed for the first time the defined distances of active site Thr1 residues between adjacent β-subunits. In this prokaryotic proteasome, the distances between active site residues are always about 30 Å, which would be enough to allow binding of peptides of eight to twelve amino acids in an extended conformation.[45] As described already, eukaryotic proteasomes contain a reduced number of proteolytically active sites (only 6 as compared to 14 in prokaryotes). Mutagenesis of active site residues in the yeast proteasome led to inactivation of four of the six active β-type subunits, β1, and β2.[75] The distance between the remaining active β5 and β5′ threonines in the mutant proteasome was measured to be about 49 Å,[63] suggesting products with an average length distribution of 15 to 18 amino acids, if indeed the distances between adjacent active sites were defining the product size (Figure 5c1). Interestingly, the mutant proteasome degraded yeast enolase, a commonly used thermolabile proteasomal substrate, to oligopeptides with an average length of 8 to 13 amino acids, similar to wild type proteasome.[76] As expected, the fragments produced by the double mutant revealed a processive degradation mechanism. The differences observed in the cleavage pattern as compared to wild type proteasomes were due to the fact that the mutant was only able to cleave at the chymotryptic-like active sites. Surprisingly, the turnover rates of wild type and mutant proteasomes were very similar, suggesting that the number of proteolytically active sites in proteasomes is not a limiting factor for proteolysis.[77,78] Recent studies on distinct proteolytically active centers demonstrated that they function independently and their relative importance varies widely with the substrate.[79] Mutational studies also excluded the presence of additional non-Thr1 endopeptidase cleavage sites in proteasomes and revealed that partially processed propeptides of the β-subunits rearrange to their final locations after they have been hydrolyzed and proteasome maturation is completed.[46,47,63,64,80] Structural and functional experiments showed that proteolytic substrates dock in specific channels near active centers, which exhibit binding sites for peptides seven to nine amino acids long[63,76] (Figure 4b). Generally, the maximum likelihood of substrate cleavage depends on its mean residence time at the proteolytically active sites, so that the product cleavage pattern is directly related to the affinity of the substrates for the individual binding clefts. Consistently, the different cleavage specificities of the active subunits of the eukaryotic proteasomes derive only from the various compositions of their binding pockets (Figure 4d).[50] It must be emphasized that the proteasome complex cannot be considered as a simple collection of various proteolytic specificities and the characteristics of generated products are determined by the overall structure of the proteolytic chamber. Nevertheless, the experimental evidence argues against the existence of allosteric interactions between the active sites for product formation: comparison of the crystal structures of proteasome mutants with the wild type shows no significant changes of subunit positions or backbone structure. Furthermore, the covalent binding of subunit specific inhibitors has no influence on the remaining active sites and does not cause noticeable structural changes (see also below).[81]

3.4. Proteasomal Substrate Binding Channels

Eukaryotic proteasomes contain different protease activities and are able to cleave almost after each amino acid.[82,83] Experiments with fluorogenic substrates demonstrated that proteasomes carry at least five distinct cleavage preferences, named chymotryptic-like, tryptic-like, caspase-like, branched chain amino acid preferring (BrAAP), and small neutral amino acid preferring (SNAAP) activity. Mutational and structural studies contributed to the determination of the proteolytic role of each β-subunit.[50,63,75] All the active centers harbor an N-terminal threonine residue acting as the nucleophile, but the distinct preferences of the various active subunits were shown to be determined solely by the composition of the substrate binding pockets, which are termed nonprimed (S1, S2, S3, ..., S*n*) and primed (S1′, S2′, S3′, ..., S*n*′) sites, depending on their proximity to the active centers. Residues in the substrate, which interact with the proteasomal specificity pockets, are referred to as P1, P2, P3, ..., P*n* and P1′, P2′, P3′, ..., P*n*′, accordingly (Figure 4b).

Proteasomal S1 specificity pockets, which were originally thought to exclusively determine the cleavage preference of the active sites, are mainly formed by residue 45 of the corresponding β-subunit (Figure 4d). Additionally, adjacent subunits in the β-rings contribute to the architecture of the S1 pockets and modulate their character. Arg45 in the S1 pocket of subunit β1 preferentially interacts with a glutamate residue in the P1 position and therefore provides for the caspase-like activity of this subunit's active site. These structural observations were confirmed by mutational analysis.[84,85] However, experiments with proteolytic degradation of yeast enolase have revealed that subunit β1 possesses, besides its caspase-like activity, also limited BrAAP activity.[63] Subunit β2 has a glycine residue in position 45 and, consequently, a spacious S1 pocket confined at its bottom by Glu53. This subunit is well suited for accepting very large P1 residues of basic character and, therefore, exhibits tryptic-

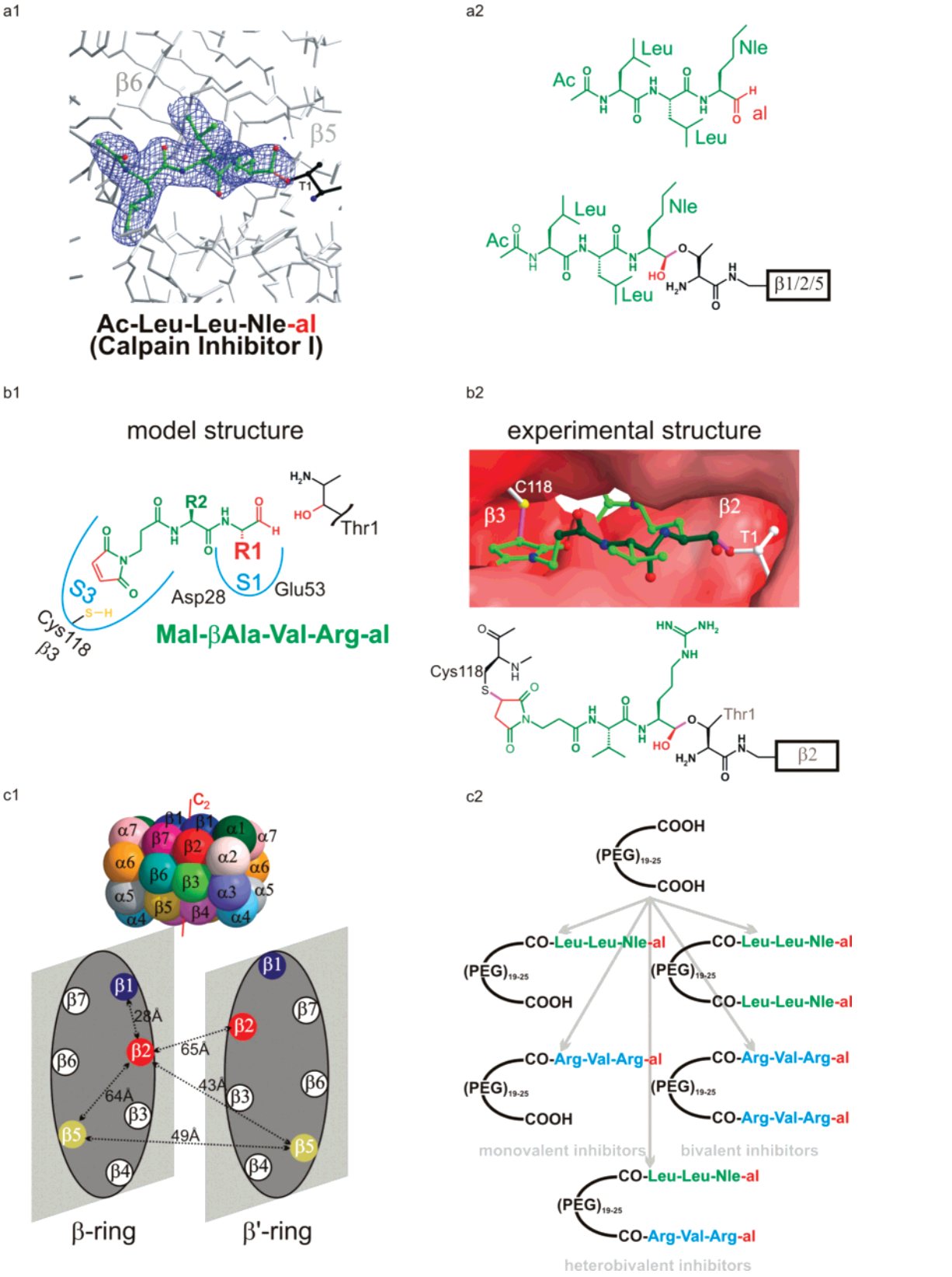

Figure 5. Yeast proteasome in complex with synthetic aldehyde inhibitors. (a1) Covalent linkage of calpain inhibitor I to the chymotryptic-like active site. The inhibitor is shown in green, and subunits $\beta5$ and $\beta6$ are shown in white and gray, respectively. The electron density map (blue) is shown for the inhibitor bound to Thr1 (black); the covalent bond is shown in magenta.[45,50] (a2**)** Structure of calpain inhibitor I. The inhibitor is shown in green, and the functional aldehyde group is shown in red. Subunits' $\beta1/2/5$ active site Thr1 residues are shown in black. (b**)** Modeled (b1) and experimentally confirmed (b2) covalent binding of Mal-βAla-Val-Arg-al, selective bivalent inhibitor to subunit $\beta2$. Residues Asp28 and Glu53 of subunit $\beta2$ are involved in formation of the tryptic-like cleavage site, and residue Cys118 of subunit $\beta3$ is mainly responsible for the character of the S3 specificity pocket. (b2) Surface representation of the tryptic-like active site complexed with the inhibitor Mal-βAla-Val-Arg-al (shown as a ball-and-stick model). (c**)** Bivalency as a principle for proteasome inhibition. (c1) Schematic representation of the central β and β' rings of the yeast proteasome with selected distances between active sites according to the crystal structure. (c2) Strategy of creation of monovalent, bivalent, and heterobivalent PEG−peptide aldehyde conjugates.[117]

like activity. The chymotryptic-like activity is attributed to subunit β5, which has its S1 pocket shaped in particular by Met45. However, mutational analysis showed that subunit β5 also has the tendency to cleave after small neutral and branched side chains, assigning additionally BrAAP and SNAAP activity to this subunit.[63]

3.5. Generation of Antigenic Peptides by Proteasomal Immuno Subunits

In mammalian proteasomes, constitutive proteolytic subunits are replaced by immuno subunits upon γ-interferon induction. That allows cells to improve control over the quantity and quality of antigenic peptides presented by the MHC class I molecules on the cell surface.[53,54,86] Introduction of immuno subunits[87−90] leads to the generation of oligopeptides, which have higher affinity to bind to MHC class I receptors.[91,92] Peptides effectively presented by MHC class I molecules usually are 8−9 amino acids in size, which represents the typical product length generated by all 20S proteasomes.[93] Structural superposition shows that the topology of MHC class I molecule bound peptides matches quite well with the propeptides of the proteasomal active sites, which may be regarded as the prototype of the optimal substrates, indicating possible coevolution of MHC molecules and proteasomal ligand binding sites (Figure 4f).[94] Antigenic peptides predominantly exhibit basic or hydrophobic C-terminal anchor residues,[95,96] required for tight binding and stabilization of MHC class I molecules. The specificity pockets of proteasomal chymotryptic- and tryptic-like active sites have a suitable residue composition for producing antigenic peptides, but the binding pocket of the caspase-like active site, located at subunit β1, does not. Interestingly, it is subunit β1 in which most residues forming the S1 specificity pocket have been replaced in β1i.[50] Subunit β1i shows two major differences in its primary sequence as compared to β1: Thr31 is changed to phenylalanine and Arg45 to leucine (Figure 3). Modeling experiments with wild type yeast proteasome showed that these two substitutions reduce the size of the S1 pocket and suggest that the caspase-like activity of this subunit is altered to chymotryptic-like activity. This explains the earlier results showing that knockout mutants of subunit β1i have a modified viral specific T-cell response and modulate the peptidase activity of the proteasome.[97,98] Similar modeling of subunits β2i and β5i does not indicate substantial modifications in the arrangement and specificities of their S1 pockets.[50] However, *in vivo* experiments in mice show that mutants lacking these two immuno subunits have severe defects in MHC class I presentation.[87] The crystal structure of the inhibitor homobelactosin C complexed to the yeast proteasome offered an explanation, since the structure helped to identify the primed proteasomal substrate binding channel (Figure 4b and Figure 7c).[94] Comparison of the primary sequences of human subunits β5 and β5i revealed two alterations: Ser115 and Glu116 of the constitutive subunit β5 are replaced by glutamate and histidine in subunit β5i, respectively (Figure 3). These conformational rearrangements modify the size and polarity of the primed substrate binding channel, which have significant effects on substrate preference and result in a new product cleavage pattern. Sequence alignment of mammalian β5 and β5i subunits from different species showed strict conservation of these residues in the constitutive β5 subunits and minor species specific differences in the immuno subunit β5i, indicating a conserved principle of modulation of the proteasomal primed substrate binding channel during the immune response. Modeling experiments showed that the primed substrate binding channels of the caspase- and tryptic-like activities are compositionally strikingly similar to that of the chymotryptic-like active site, and all of them exhibit significant differences between their constitutive and γ-IFN induced versions. Cells infected with viruses contain both constitutive as well as immuno proteasomes, and cytotoxic CD8 T cells are sensitive even for single specific MHC class I−peptide complexes on the cell surface.[99] Since proteasomal β2 and β5 constitutive and immuno subunits differ only in their primed specificity channels, γ-IFN inducible replacement of these subunits will lead to an alternative substrate cleavage pattern, thus increasing the variability of the generated ligands, which are all suitable to bind to MHC class I receptors.[94]

4. Inhibitors of the Proteasome

4.1. Fundamental Characteristics of Proteasome Inhibitors

More than 90% of cell protein degradation is performed by the ubiquitin−proteasomal pathway. The proteasome is a core component of this machinery, and regulation of its activity is particularly important for the vast amount of essential biological processes. Consequently, chemical compounds inhibiting or modulating proteasomal activity have great biological significance. They can be used both as tools to investigate regulation of the ubiquitin−proteasomal system and as lead structures for design of fine-tuned proteasome inhibitors with perspectives for possible drug development.

After the discovery of proteasomes, a great variety of natural and synthetic chemical compounds were tested for their ability to inhibit different proteasomal proteolytic activities (Table 1). Classification of proteasomal inhibitors is based on their characteristic binding mode to the proteolytically active sites, specificity, and reversibility of binding. Peptide aldehydes were the first discovered inhibitors of the 20S proteasome,[100] and they are still actively investigated. Another class of proteasomal inhibitors, first discovered as inhibitors of cysteine proteases, are peptides having a vinyl sulfone functional group.[101] Peptide boronates, which are much more potent inhibitors than aldehydes and vinyl sulfones, represent the next class of inhibitors.[102] High inhibition efficiency of boronate compounds, their selectivity, and low dissociation rates put these chemical compounds in the focus of medical research and drug development. The boronate derivative bortezomib has already passed through clinical trials and represents a new drug against multiple myeloma.

Beside synthetic peptide inhibitors, there exist a variety of natural compounds blocking the proteasomal activity, with the main three groups being $\alpha'\beta'$-epoxyketones, β-lactones, and TMC-95s. The crystal structures of the proteasomes in complex with various synthetic and natural inhibitors provided valuable insights about the architecture and organization of substrate binding pockets located near proteasomal active centers. The structural information about the binding modes of different chemical compounds stimulated development of more potent inhibitors blocking the individual proteolytic activities of the proteasome. In the following sections, we will discuss the main classes of proteasomal inhibitors, focusing on the structural and chemical aspects such as binding mode, specificity, selectivity, and possible biomedical implementations.

Table 1. Major Classes of Proteasomal Inhibitors

class	compound	inhibition of proteasomal active sites [K_i (nM) for reversible inhibitors and K_{ass} (M^{-1} s^{-1}) for irreversible inhibitors] chymotrypsin-like	trypsin-like	caspase-like	other than proteasome intracellular targets (IC_{50})
		Reversible Inhibitors			
peptide aldehydes	calpain inhibitor I (Ac-Leu-Leu-nLeu-al)	140[b]	nd	nd	calpains
	calpain inhibitor II	nd	nd	nd	calpains, lysosomal enzymes
	MG132 (Z-LLL-al)	4[b]	nd	0.4	calpain, cathepsins
	PSI (Z-IE(OtBu)Al-al)	IC_{50}: 250[a]	6.5 μM[a]	nd	calpain, cathepsins
	CEP1612	nd	nd	nd	calpain, cathepsin B
	BSc2118 (Z-Leu-Asp(OtBu)-Leu-al)	IC_{50}: <60[a]	nd	nd	not tested
peptide boronates	MG262 (Z-LLL-bor)	0.02[c]	nd	nd	Lon protease from *Salmonella*[f]
	PS341 (bortezomib)	0.62[c]	nd	nd	chymotrypsin, thrombin[g]
	PS273 (MNLB)	0.15[d]	nd	nd	elastase,[h] dipeptydil protease IV[i]
		Irreversible Inhibitors			
lactacystin and derivatives	lactacystin	194	10	4.2	cathepsin A, TPPII
	β-lactone (omuralide)	IC_{50}: 57[m]	540[m]	10000[m]	cathepsin A, TPPII
	salinosporamide A	IC_{50}: 2.6[m]	4.1[m]	430[m]	
	salinosporamide B	IC_{50}: 27[m]	640[m]	1200[m]	
peptide vinyl sulfones	ZLVS (Z-Leu-Leu-Leu-vs)				
	NLVS (Nip-LLL-vs)	13400[d]	422	100	cathepsin S and B
	YLVS (YLLL-vs)	1500[d]	560	20	cathepsin S and B
	AdaAhx3-Leu-Leu-Leu-vs				cathepsin S and B
	Tyr-Leu-Leu-Leu-vs				interferon-inducible proteasome[e]
	NIP-Leu-Leu-Asn-vs				
peptide epoxyketones	dihydroeponemycin	58[j]	17[j]	175[j]	cathepsin B (very weak)
	epoxomycin	20000[j]	310[j]	43[j]	none found
	YU101 (Ac-hFLFL-ex)	166000[k]	7.1[k]	0.25[k]	not tested
	TMC-86A	IC_{50}: 5.1 μM[l]	51 μM[l]	3.7 μM[l]	not tested
	TMC-89	na	na	na	not tested
	TMC-96	IC_{50}: 2.9[l]	36[l]	3.5[l]	
		Noncovalent Reversible Inhibitors			
	TMC-95A	IC_{50}: 5.4 nM[n]	200 nM[n]	70 nM[n]	none found

[a] Figueiredo-Pereira, M. E.; Chen, W. E.; Yuan, H. M.; Wilk, S. *Arch. Biochem. Biophys.* **1995**, *317*, 69. [b] Reference 106. [c] Reference 102. [d] Grisham, M. B.; Palombella, V. J.; Elliot, P. J.; Conner, E. M.; Brand, S.; Wong, H. L.; Pien, C.; Mazzola, L. M.; Destree, A.; Parent, L.; Adams, J. *Methods Enzymol.* **1999**, *300*, 345. [e] Reference 124. [f] Frase, H.; Hudak, J.; Lee, I. *Biochemistry* **2006**, *45*, 8264. [g] Reference 135. [h] Reference 136. [i] Reference 137. [j] Reference 154. [k] Reference 145. [l] Reference 158. [m] Reference 175. [n] Reference 185.

4.2. Peptide Aldehydes

4.2.1. Discovery and Binding Mode of Aldehyde Inhibitors

The first experiments with inhibition of proteasomal activity demonstrated that the proteasome is sensitive to 3,4-dichloroisocoumarin (DCI), a specific serine protease inhibitor. However, this inhibitor only blocked the activity of the proteasome against peptides and had no effect on degradation of protein substrates.[103] Thus, it seemed that the proteasome does not belong to the classical family of serine proteases. Other protease inhibitors were tested for further investigation of the proteasomal catalytic mechanism, among them the calpain inhibitors I and II.[100] Calpain inhibitors were the first synthetic inhibitors of serine and cysteine proteases, originally created to block the activity of calpains, members of the cysteine protease family involved in several intracellular signaling pathways mediated by Ca^{2+}.[104] Both calpain inhibitors efficiently blocked the proteolytic activity of the proteasome. However, due to the high reactivity of the functional aldehyde group, calpain inhibitors lack specificity and also inhibit a broad range of different serine and cysteine proteases.[105] The first structural information of the architecture of proteasomal proteolytically active sites was obtained from the crystal structure of *Thermoplasma acidophilum* proteasome in complex with calpain inhibitor I (Ac-Leu-Leu-nLeu-al) (Figure 5a2).[45] These data revealed that proteasomes belong to a novel class of proteases which use threonine as the nucleophilic residue in their active sites. Calpain inhibitor I was found to be covalently bound to the hydroxy group of Thr1 of all proteasomal β-subunits with the formation of hemiacetal bonds (Figure 5a1). Upon binding, the inhibitor adopts a β-conformation and fills the gap between strands S2 and S3 by forming hydrogen bonds with residues 20, 21, and 47 and generating an antiparallel β-sheet structure. The norleucine side chain of the inhibitor projects into the S1 pocket that opens sidewise toward a side channel leading to the surface of the molecule. The leucine side chain at P2 is not in contact with the protein, whereas the leucine side chain at P3 is in close contact with residues of the adjacent β-subunit.

In eukaryotic proteasomes, only three β-type subunits, β1, β2, and β5, are proteolytically active, whereas the others remain inactive (see also section 3.2). Although the proteolytic mechanisms of all active sites are identical, calpain inhibitor I binds with the highest affinity (IC_{50} of 2.1 μM) to subunit β5, carrying the chymotryptic-like active site, and has a low effect (IC_{50} values > 100 μM) on tryptic- and caspase-like activities (subunits β2 and β1, respectively). However, the crystal structure analysis of the yeast proteasome in complex with calpain inhibitor I showed binding of the inhibitor molecule to all active centers,[50] which can be explained by the high concentration of the compound used in the soaking buffer. Similar to what has been observed for the *Thermoplasma* proteasome, the inhibitor forms a hemiacetal bond with all active Thr1O$^{\gamma}$s. These structural data helped to identify the specificity pockets in eukaryotic

proteasomes and revealed that the active sites of subunits β1, β2, and β5 differ significantly in the architecture of their S1 and S3 pockets (see also section 3.4). The bottom of the S1 pocket, which appears largely to determine its substrate preference, is formed by residue 45 of the β-subunit carrying the proteolytically active site. The S3 pocket is formed by residues of the adjacent β-subunit. The chymotryptic-like active site, which shows the highest affinity for calpain inhibitor I, contains in its S1 pocket Met45 surrounded by the hydrophobic residues of subunit β5, which stabilize the norleucine side chain of the inhibitor by hydrophobic interactions. The S3 pocket of the chymotryptic-like active site, which is formed by charged residues of subunits β5 and β6, is not involved in binding of the Leu P3 side chain of the inhibitor. The tryptic-like active site possesses spacious overall negatively charged S1 and S3 specificity pockets, which do not contribute to the stabilization of the norleucine and the P3 Leu side chains of the inhibitor. The caspase-like active site has the smallest S1 specificity pocket, which is positively charged due to the presence of Arg45. Thus, the norleucine side chain of the inhibitor has to adopt an unfavorable conformation in order to fit into the pocket. Analysis of the electron density revealed that the guanidinium side chain of Arg45 is associated with a counterion, compensating for the unbalanced positive charge. The small S3 specificity pocket of the caspase-like active site carries charged side chains, which are not stabilizing the inhibitor. These findings explain the high preference of calpain inhibitor I for the chymotryptic-like active site. As already mentioned earlier, the proteolytic activities of the proteasome, which differ in their kinetics, pH optimums, and inhibitor sensitivities, were originally described as chymotryptic-, tryptic-, and caspase-like activities. The fact that calpain inhibitor I was found to be bound to all active sites simultaneously demonstrated that this classification does not exactly reflect their true proteolytic nature. The low selectivity of calpain inhibitor I is explained by the presence of a highly reactive aldehyde group, enabling the inhibitor to bind to all proteolytically active sites. This inhibitor has very low selectivity for proteasome and is 25-fold more potent against cathepsin B and calpain.[106] Further research in combination with structural and functional data on mammalian and yeast proteasomes was required for modeling of more selective chemical compounds inhibiting specific proteolytically active sites.

4.2.2. Commonly Used Aldehyde Inhibitors

Generally, aldehyde inhibitors enter cells rapidly and their effect is reversible. These inhibitors have fast dissociation rates, they are rapidly oxidized in inactive carbonic acids, and they are transported out of cells by the multidrug resistance system carrier.[105] Consequently, in experiments involving cultured mammalian or yeast cells, the effects of these inhibitors could be rapidly reversed by removal of the inhibitor.[107] Up to date, many peptide aldehydes have been designed and synthesized, and some of them are now used widely for proteasome inhibition experiments.[108] For example, MG132 (Z-Leu−Leu-Leu-al) not only is significantly more potent against the proteasome than calpain inhibitor I[109] but also is much more selective, as shown by the fact that inhibition of calpains and cathepsins requires at least a 10-fold higher concentration of this compound.[110] The critical difference between calpain inhibitor I and MG132 is that the P1 site of the latter carries a leucine side chain, which is more favorable for ligand stabilization. Another peptide aldehyde, PSI (Z-Ile-Glu(Ot-Bu)-Ala-Leu-al) inhibits the proteasome 10-fold better than calpain but is still less potent than MG132.[111] A dipeptide aldehyde CEP1612 appears to be at least as good as MG132 in terms of potency and selectivity.[108] So far, there are no structural data available for the previously described calpain inhibitor I analogues in complex with proteasomes. Since adaptation and movement of the ligand are crucial for stabilizing the ligand in its bound state and have significant effects on IC_{50} values, structural information on the flexibility of residues and the space restrictions of the protein ligand binding pockets can be used for structure-based design of inhibitor side chains in order to increase their affinity for specific active sites.

As revealed by crystal structure analysis, proteasomes do not possess S2 specificity pockets.[45,50] This feature provides an advantage in the inhibitor design: bulky and space demanding residues can be introduced in the P2 site, which enhances the specificity of the inhibitor for proteasomes and prevents unspecific inhibition of other proteases which have space limiting S2 pockets.[112] The characteristics and specificities of MG132 stimulated the design of potent but more specific 20S proteasome inhibitors varying in the composition of their P2 sites.[113] BSc2118 (Z-Leu-Asp(OtBu)-Leu-al) has proven to be the most potent (IC_{50} < 60 nM) of these compounds due to its spacious P2 site carrying, besides the aspartate, a tertiary butyl moiety. The crystal structure analysis of the proteasome in complex with BSc2118 confirmed that though this space demanding side chain is not involved in ligand−protein contacts, it restricts the flexibility of the ligand. This conformational feature additionally prevents the inhibitor from binding to the active sites of most other proteases harboring distinct S2 pockets.

4.2.3. Structure-Based Improvement of Aldehyde Inhibitors

So far, structural data have been used for verification of theoretical speculations about the inhibitor binding mode. A more efficient approach would be to take advantage of the available structural information for modeling of new specific inhibitors, selective for single proteasomal proteolytically active sites. Only limited substrate specificity characterizes the active sites of subunits β1, β2, and β5, responsible for caspase-, tryptic- and chymotryptic-like activities, which makes substrate-based design of selective inhibitors extremely difficult. The structural data of the eukaryotic proteasome provided insights for the development of new inhibitors, which have several docking sites for covalent binding to the protein. The traditional classification of proteasomal cleavage preferences is based only on experimental data with chromogenic peptides, which, however, do not represent natural proteasomal substrates.[114] Structural information on the architecture of proteasomal substrate binding channels has proven to be valuable for ligand modeling in order to increase the affinity of the inhibitors for specific active sites. The first insights were obtained when the P3 site of calpain inhibitor I was redesigned in order to test its influence on the inhibition efficiency. A maleinimide group, matching the configuration of the S3 binding pocket of the tryptic-like active site (which contains Cys118 of subunit β3), was introduced to the P3 site of the calpain inhibitor I, in order to test the contribution of the S3 pockets to the ligand stabilization.[115] Structure-based modeling was required to measure the characteristic distance between the maleinimide side chain of the inhibitor

and the thiol group of the P3 pocket (Figure 5b1). The calculations showed that the βAla-maleinimide would meet these expectations. The inhibitor was supposed to bind covalently with its maleinimide group in the P3 site bound to the S3 thiol group of Cys118 and with its carboxy terminal aldehyde group for hemiacetal formation bound to the Thr1O$^{\gamma}$ of subunit β2 (tryptic-like activity). Thus, the first inhibitor was designed which carried the P1 site for chymotryptic-like activity and the P3 site for tryptic-like activity. The results of the inhibition experiments turned out to be surprising: as compared to calpain inhibitor I (most selective for the chymotryptic-like activity), the newly designed inhibitor showed a 10-fold increase of inhibition efficiency for tryptic-like activity, whereas its efficiency for chymotryptic-like activity severely decreased.[115] These results demonstrated for the first time that the binding efficiency of the ligand can be altered by manipulations exclusively with its P3 site, and they opened new perspectives for design and synthesis of specific inhibitors for single proteasomal subunits. Moreover, it was shown that traditional classification of the distinct proteasomal active sites, which is still commonly used, does not fully reflect actual cleavage preferences. From analysis of the crystal structure of the calpain inhibitor I bound to the various proteasomal active sites, it became clear that the norleucine side chain in P1 is not suitable for ligand stabilization in the S1 pocket of the tryptic-like active site, which is spacious and carries an overall negative charge. Thus, in the next step, the norleucine side chain was replaced with positively charged residues (Lys or Arg). The compound carrying lysine instead of norleucine demonstrated a 4-fold increase of the inhibition efficiency, whereas the compound with the arginine substitution was 25-fold more potent ($IC_{50} < 0.5\ \mu M$).[115] These significant differences in inhibition rates could not be explained from the structural data of the proteasome−Mal-β-Ala-Val-Arg-al complex, since molecules in the crystal are rigidly packed and crystallization buffer conditions usually do not represent an optimal enzyme environment. However, the crystallographic data has proven to be important for the determination of the optimal spacing of the maleinimide group from the P2−P1 dipeptide aldehyde. As described above, the side chain of Cys118 of subunit β3 protrudes into the S3 subside of the tryptic-like active site. The location of this residue was exploited for the rational design of bivalent inhibitors containing a maleinimide moiety at the P3 position for covalent linkage to the thiol group and the carboxy terminal aldehyde group for hemiacetal formation with Thr1O$^{\gamma}$ of the active site. These structurally based predictions were confirmed by analysis of the crystal structure of the yeast proteasome−Mal-βAla-Val-Arg-al complex. It was seen that the inhibitor molecule only binds to subunit β2 by hemiacetal formation (Figure 5b2). The presence of the covalent bond between the maleinimide and the Cys118 residue of subunit β3 has been confirmed. Remarkably, the IC_{50} value of Mal-βAla-Val-Arg-al for subunit β2 is 0.5 μM, which is 400 times less as compared to the IC_{50} value of calpain inhibitor I (200 μM). Thus, Mal-βAla-Val-Arg-al represents a new type of inhibitor that is highly selective for the tryptic-like activity. The inactivation potencies of the maleinimide dipeptide aldehydes were found to depend strongly upon the side chain of the carboxy terminal aldehyde group, which interacts with residues forming the S1 specificity pocket. Binding of the inhibitor starts with hemiacetal formation, followed by juxtaposition of the maleinimide group at the S3 site for reaction with the thiol functional group of Cys118. The crystallographic data of the proteasome−inhibitor complex revealed that despite the presence of numerous accessible cysteine residues and a more than 1000-fold excess of the maleinimide compound during crystal soaking, the inhibitor molecules were only bound to the nucleophilic Thr1O$^{\gamma}$ of subunit β2. Since Cys118 is conserved in all eukaryotic proteasomes, the new inhibitor promises to be an efficient tool for investigation of substrate degradation mechanisms. However, the reactivity of the maleinimide group toward free thiols such as glutathione limits the use of the inhibitor only to *in vitro* assays.[116]

4.2.4. Bi- and Multivalency as a Strategy To Increase Inhibitor Potency

Previously described data stimulated further development of specific inhibitors for single proteolytically active sites of proteasomes. The unique topography of the six proteolytically active subunits in the central chamber of eukaryotic proteasomes defines the distances between the active site Thr1-residues (Figure 5c1). Using the known proteasomal layout, new bi- or multivalent proteasome inhibitors have been designed. These inhibitors contain an oligomeric spacer of appropriate length, linking two monovalent binding head groups to each other, with the formation of homo- or heterobivalent compounds.[117] The spacer must be unable to form any secondary structure, so that the inhibitor can reach the proteasomal central cavity. Unfolded peptides like gastrin (17mer) or secretin (27mer) were found to be rapidly degraded by the proteasome and were, therefore, unsuitable for the role of spacer elements. Polyethylene glycol (PEG) was selected as a possible spacer, since it is a linear, flexible, soluble, and protease resistant polymer, which mimics unfolded peptide chains. Furthermore, the PEG spacer is hydrophilic and, therefore, prevents formation of hydrophobic cores, which would disturb the molecule entering the proteasome. Spacer lengths for the various bifunctional inhibitors were chosen on the basis of the proteasomal inter- and intra-ring distances. Finally, the N-termini of two calpain inhibitor I molecules were linked to the related PEG spacer, resulting in a bivalent protease resistant proteasome inhibitor (Figure 5c2). As expected, due to the flexibility of the PEG linker region, the crystal structure analysis of the proteasome−inhibitor complexes did not reveal a conformationally restricted PEG moiety in any part of the density. Kinetic measurements of the proteolytic activity of the yeast proteasome showed that the bivalent inhibitors have IC_{50} values in the low nanomolar range ($IC_{50} < 0.02\ \mu M$). In contrast, its monovalent analogue has 100-fold higher IC_{50} values. Thus, the inhibition potency of the bivalent inhibitor was increased by 2 orders of magnitude as compared to that of its monovalent analogue. To prove if the principle of bivalent inhibition applies generally, two molecules of a newly designed aldehyde inhibitor for the tryptic-like activity (Ac-Arg-Leu-Arg-al) were covalently bound through the PEG spacer. The effect of the bivalent inhibitor was the same as has been observed for the bivalent calpain inhibitor I (IC_{50} increase 100-fold). Interestingly, improved inhibition was achieved by using a heterogeneous population of polymeric spacers with a length distribution from 19 to 25 monomers to bridge various active sites. The next step was to design a heterobivalent inhibitor molecule with two different head groups connected with a PEG spacer for simultaneous inactivation of two distinct proteolytically active subunits (Figure 5c2). The geometric arrangement of the six active

sites in the two inner β-rings allows inhibition of two different activities with one molecule. In the case of homobivalent inhibitors, one molecule can neutralize only the active sites of symmetry related identical active subunits ($\beta1-\beta1$, $\beta2-\beta2$, $\beta5-\beta5$). The advantage of the heterobivalet inhibitor is that two molecules of the ligand can block two different proteasomal activities simultaneously. This hypothesis was confirmed experimentally by designing a heterobivalent inhibitor containing as head groups the tripeptide aldehydes calpain inhibitor I and Arg-Val-Arg-al. As expected, tryptic- and chymotryptic-like activities were inhibited. The inhibitory potencies against both activities were similar to those of the homobivalent inhibitors.[117] The experimental functional data confirm the hypothesis of the bivalent binding, since the occupation of all six active sites is expected to occur in both the intra- and inter-ring modes, providing the spacer length is sufficient for all the possible bridging within maximal distances of approximately 65 Å (PEG spacer > 19-mer). The crystal structure analysis of the proteasome in complex with homo- and heterobivalent inhibitors clearly defined the electron density of the tripeptide aldehyde and the beginning of the PEG spacer, whereas the remaining part of the spacer, which was not conformationally restricted, could not be seen in the electron density.

Multivalency as a tool of enhancing affinity has been originally established in chelate chemistry.[118,119] This universal principle also exists in nature, being ubiquitously exploited to enhance selectivity and avidity in molecular recognition processes, which can be seen in the example of antibodies (multivalent representation of Fab fragments[120]) as well as in the broad range of enzymes catalyzing all kinds of chemical reactions (first described in the structural analysis of hemoglobin[121]). The general principle of bivalency of proteasome inhibitors is not limited to the use of peptide aldehydes as binding head groups. By combination of more potent and selective inhibitor head groups (see below), it should be possible to create specific inhibitors of the proteasome acting in the picomolar range. The question of whether PEG-linked bivalent inhibitors retain membrane permeability for entering the intracellular space has not yet been answered. However, the advantages of PEG spacers are their nontoxicity and nonimmunogenicity. Besides, PEG spacers increase the solubility of the inhibitors and can facilitate their transfer through the cellular membrane. These features make PEG-based bivalent inhibitors promising compounds for further investigations and biomedical applications.

4.3. Peptide Vinyl Sulfones

Peptides possessing a vinyl sulfone moiety represent another class of proteasome inhibitors.[122] These compounds bind to proteasomes irreversibly but are less reactive than aldehydes. Vinyl sulfones act as Michael acceptors for soft nucleophiles such as thiols, leading to the formation of a covalent bond (Figure 6a2). They do not inhibit the activity of serine proteases, but they show high specificity for intracellular cysteine proteases such as cathepsins, which applies certain restrictions to their application *in vivo*, similar as peptide aldehydes. The selectivity of inhibition by vinyl sulfones can be modified by manipulations of the peptide part of these inhibitors. For example, replacement of the benzyloxycarbonyl (Z-protecting) group in ZLVS (Z-Leu-Leu-Leu-vs), a vinyl sulfone analogue of MG132, by the 3-nitro-4-hydroxy-5-iodophenylacetate (NIP) group to generate NLVS significantly reduces the inhibition of cathepsin B and cathepsin S.[123] Vinyl sulfones are easier to synthesize than other irreversible inhibitors of the proteasome,[112] but the main advantage of these covalent inhibitors is that they can be used as sensitive active site probes for mechanistic studies of proteasomes in different tissues and cells.[124] For instance, broad-spectrum, irreversible vinyl sulfones have been used in the profiling of proteolytically active subunits of the proteasome.[125] The inhibitors were labeled with either a radioisotope, a biotin moiety, or a fluorescent tag, to allow visualization, isolation, and quantification of distinct proteasomal subunits.

The most potent peptide-based vinyl sulfone (AdaAhx$_3$-Leu−Leu-Leu-vs), which irreversibly and specifically inhibits proteasomal activity, has the unique quality of binding to all proteolytically active β-subunits of both the constitutive and the γ-interferon-inducible immuno subunits with approximately equal efficiency. Modification of AdaAhx$_3$-Leu-Leu-Leu-vs with an azid group interferes neither with the inhibition profile nor with the cell permeability of the compound.[124] Incubation of cells or cellular extracts with vinyl sulfone compounds results in the covalent attachment of inhibitor molecules to the active subunits of the proteasome, which can be identified by comparing the mobility of proteasomal subunits on 2D gels. Thus, it is possible to label whole cells with this inhibitor by decorating proteasomal active β-subunits: after cell lysis and denaturation of the cellular protein content, the azido group is visualized by modification with an easily detectable biotinylated phosphane reagent.[126,127] So far, the most widely used vinyl sulfones, which react with all three distinct proteasomal active sites, are [^{125}I]Tyr-Leu-Leu-Leu-vs,[123,128] NIP-Leu-Leu-Asn-vs,[112] and Ada-[^{125}I]Tyr-Ahx$_3$-Leu-Leu-Leu-vs.[124,125]

Several elements that can be used to control the selectivity of synthetic inhibitors have been identified during scanning of libraries of peptide-based covalent proteasome inhibitors.[50,115,117,129] Initial screenings identified the vinyl sulfone Ac-YLLN-vs as a compound which blocks all proteasomal active sites. A further random positional search for selective vinyl sulfones identified Ac-PRLN-vs as an inhibitor specific for subunit $\beta2$.[112] Remarkably, in contrast to Ac-YLLN-vs, this inhibitor is highly selective, although these two compounds vary only in their P3 and P4 positions. The crystal structures of the yeast proteasome in complex with these two vinyl sulfones revealed that the inhibitors' identical P1 sites adopt the same conformation in the S1 pockets. However, it is the favorable interaction between the P3 residue and the S3 pocket, generated at the interface of neighboring β-subunits, which explains their selectivity (Figure 6a1).[130] These results are in accord with experimental data obtained for previously described peptide aldehydes[115] and demonstrate once again the feasibility of inhibitors, which specificities can be controlled predominantly by modifications of their P3 sites. Nevertheless, strong interactions at P1 may overcome the need for a favorable P3 residue. For, example, MG132 has been reported to specifically bind to subunit $\beta5$ due to its characteristic P1 site, and there exist many more examples (see below). This information, combined with findings of the importance of the P3 pocket, may facilitate the further improvement of proteasomal inhibitors with tunable selectivity for each of the active sites.

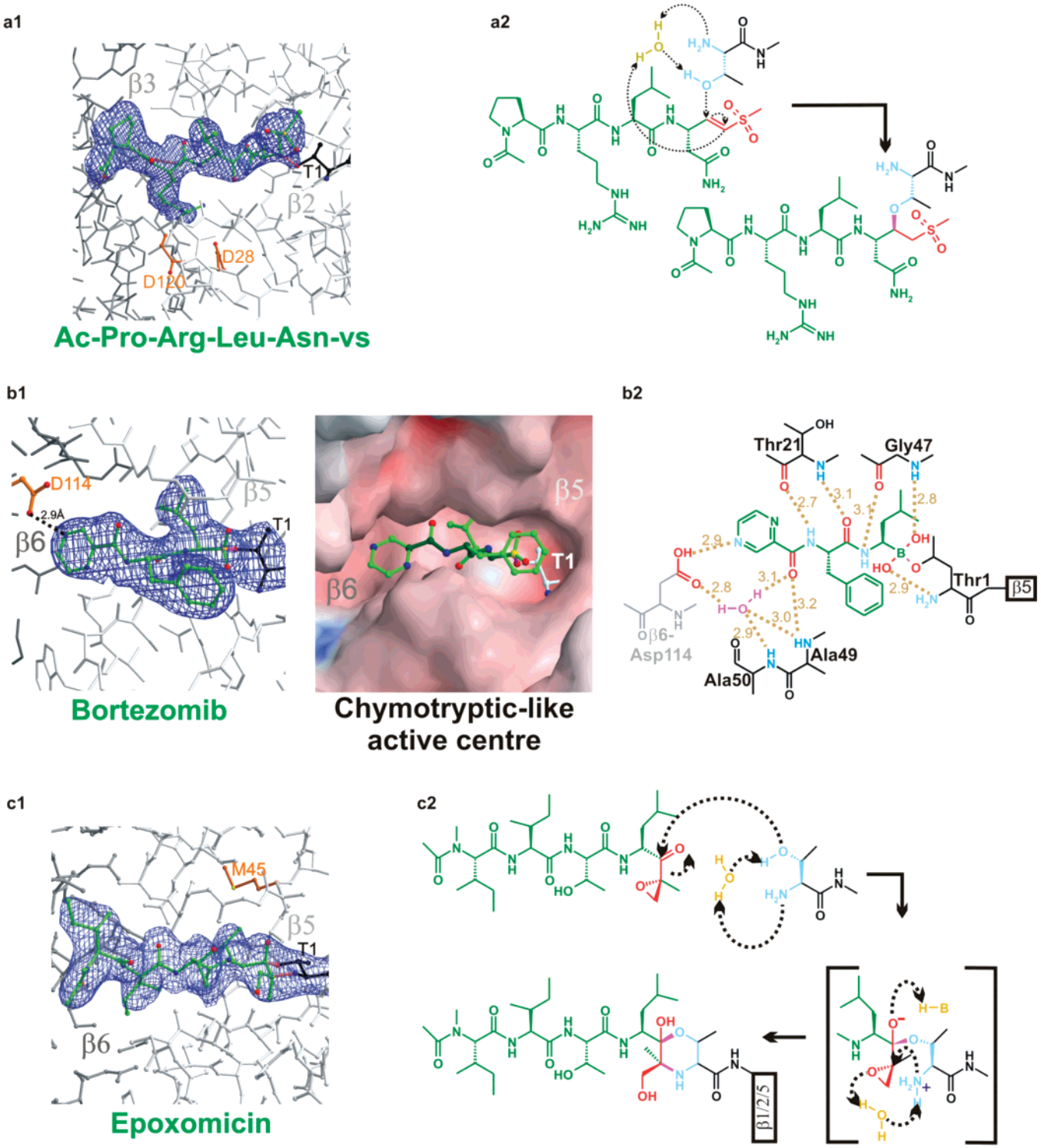

Figure 6. Yeast proteasome catalytic subunits in complex with synthetic and natural inhibitors. Subunits forming active sites and their neighboring subunits are white and gray, respectively, inhibitors are presented in green, and the functional reaction groups are depicted in red. The covalent linkages of the inhibitory compounds with the proteasomal subunits are drawn in magenta. Electron density maps (blue) are only shown for the inhibitory molecules bound to Thr1 (black). Apart from the bound inhibitor molecules, structural changes were only noted in the residues of the specificity pockets (orange). (a1**)** Ac-Pro-Arg-Leu-Asn-vs, a specific vinyl sulfone inhibitor covalently bound to subunit β2. Favorable hydrogen bonds between Asp28 of subunit β2 and Cys118 and Asp120 of subunit β3 within the walls of the S3 pocket are orange. (a2**)** The mechanism follows a typical Michael addition reaction, with irreversible binding of the vinyl sulfone inhibitor to the active site Thr1.[130] (b1**)** Chymotryptic-like active site of the yeast proteasome (ball-and-stick model and surface charge representation) in complex with bortezomib. (b2**)** Schematic representation of bortezomib bound to the proteasomal tryptic-like active site. Hydrogen bonds with correlated distances in angstroms are shown as brown dashed lines. The proteasomal residue responsible for the character and binding mode to the P3-pyrazyl-side chain of the inhibitor is located at the adjacent β-type subunit and colored in gray. The nucleophilic water molecule forming tight hydrogen bonds to the protein is depicted in magenta, and the inhibitor is shown in green.[140] (c1**)** Electron density map of epoxomicin bound to subunit β5. (c2**)** Schematic representation of the proposed morpholino derivative adduct formation mechanism. Binding of epoxomicin to the proteasome results in formation of a morpholino adduct between the epoxyketone pharmacophore and the active site amino terminal Thr1. Nucleophilic attack by Thr1O$^{\gamma}$ on epoxomicin results in hemiacetal formation followed by subsequent cyclization of Thr1N onto the epoxide, resulting in an inversion of C2 and formation of the morpholino adduct. Candidate residues for H−B and B^{-} are the Thr1 amino terminus, a bound water molecule, and invariant Ser129O$^{\gamma}$.[129]

4.4. Peptide Boronates

4.4.1. General Characteristics of Boronic Acid Derivatives as Proteasomal Inhibitors

Peptide boronates are much more potent inhibitors of the proteasome and have much slower dissociation rates than proteasome aldehyde adducts. For example, the boronate analogue of MG132, Z-Leu-Leu-Leu-boronate (MG262) has a 100-fold lower IC_{50} with an impressive K_i of 18 pM.[102] Furthermore, it turned out that dipeptide boronate derivatives are suitable for applications *in vivo*, being bioavailable and relatively stable under physiological conditions.[131] Derivatives of peptide boronates were used as fluorescent probes (morpholino-naphthylalanine-Leu-boronate [PS-273]; dansyl-Phe-Leu-boronate [DFLB])[132] to analyze proteasomal catalytic activity in living cells.[133,134] Boronic acid peptides have been shown also to inhibit serine proteases such as thrombin,[135] elastase,[136] and dipeptidyl protease IV,[137] but unlike aldehydes and vinyl sulfones, boronates are poor inhibitors of cysteine proteases, due to the weak interactions between sulfur and boron atoms.[102] Their selectivity makes boronic acid derivatives attractive candidates for drug development. Dipeptidyl boronate *N*-(4-morpholino)carbonyl-β-(1-naphthyl)-L-alanine-L-leucine boronic acid (MLN-273) has been shown to inhibit the activity of the proteasome from *Mycobacterium tuberculosis*[138] and potentially can be used for sensitizing the pathogenic molecule to the immune system. Another boronic acid dipeptide derivative, PS-341, later renamed to bortezomib, also demonstrates a high degree of selectivity for the proteasome (K_i < 0.6 nM).[139] An extensive investigation of bortezomib could not identify other targets of this inhibitor.[131] The boronic acid moiety of bortezomib ensures its increased specificity for the proteasome, in contrast to earlier generations of synthetic inhibitors such as peptide aldehydes, which show cross-reactivity toward cysteine proteases and low metabolic stability.[100] The boronic acid core ensures high affinity for hard oxygen nucleophiles and not for soft cysteine nucleophiles, according to the Lewis hard−soft acid−base principle.

4.4.2. Mode of Action: The Boronic Acid Moiety

Under physiological conditions, bortezomib preferentially targets the proteasomal β5 active site, and to a lesser extent the β1 site, while the β2 site is left relatively untouched (β5 > β1 ≫ β2).[134] Analysis of the structure of the yeast proteasome complexed with bortezomib shows all active sites occupied by the inhibitor, which is most likely due to the high concentrations of the ligand (10 mM) used for crystal soaking.[140] As has been described before, specificity pockets of individual active subunits do differ not only in their surface charge pattern but also in their overall architecture. Nevertheless, the binding mode of bortezomib and its conformation in all three subunits are identical. In its bound form, bortezomib adopts an antiparallel β-sheet conformation, similar to what has been described for calpain inhibitor I, filling the gap between strands of S2 and S4. The binding affinities of bortezomib are different for distinct active sites, due to interactions of the individual side chains of the inhibitor with the distinct protein specificity pockets (Figure 6b2). As expected, the boron atom covalently interacts with the nucleophilic oxygen lone pair of Thr1Oγ, while Gly47N, stabilizing the oxyanion hole, is hydrogen bridged to one of the acidic boronate hydroxyl groups. The tetrahedral boronate adduct is, furthermore, stabilized by a second acidic boronate hydroxyl moiety, which hydrogen bridges the N-terminal threonine amine atom. As previously mentioned, boronic acid derivatives, and particularly peptide boronates, are well-known inhibitors of serine proteases.[141] Crystal structure elucidation and NMR characterization of the trypsin−boronic acid complex have revealed a covalent binding of the nucleophilic Ser195O$^{\gamma}$ to the boronic acid moiety, resulting in a serine boronate tetrahedral transition state complex.[142−144] Compared to the cases of serine proteases, the proteasomal active site Thr1N additionally forms a tight hydrogen bridge to one of the boronate hydroxyl groups, further stabilizing the protein−ligand complex, explaining the high affinity of boronic ligands for Ntn-hydrolases.[140]

4.4.3. Binding Specificity of Bortezomib

In vivo experiments indicated that bortezomib binds covalently with the highest affinity to subunit β5.[134] The crystallographic analysis confirmed these results and revealed a structural rearrangement of the side chain of Met45 of subunit β5.[140] As already discussed, Met45 is involved in key enzyme−substrate interactions, in particular those required for hydrolysis of hydrophobic peptide bonds. Compared to the crystal structure of the native unliganded proteasome in a proteasome−bortezomib complex, the P1 leucine side chain of bortezomib shifts the side chain of Met45 from its original position by 2.7 Å toward Ile35. This structural rearrangement enlarges the S1 specificity pocket, engaging an induced fit, similar to what has been observed for calpain inhibitor I[50] and epoxomicin.[129] Although the flexibility of side chains makes it difficult to predict optimal substitution at this site, the concerted movements upon binding of bortezomib allow additional hydrophobic interactions of the P1 leucine side chain of the inhibitor with residues of the S1 pocket, further stabilizing the ligand-bound state (Figure 6b1). Bortezomib also shows some *in vivo* activity to inhibit the caspase-like site of subunit β1, which predominantly cleaves peptide bonds after acidic residues but also has limited ability to cleave after branched chain amino acids.[63,76] In the proteasome−bortezomib crystal structure, the S1 specificity pocket of subunit β1, positively charged by Arg45, is neutralized by a counterion, adapting to the P1 leucine side chain of the inhibitor without conformational rearrangements, which is in accord with the functional data. As found experimentally, bortezomib does not block the proteasomal β2 active site *in vivo*, even in the high micromolar range. However, the crystallographic data exhibit a clear electron density of the compound covalently bound to subunit β2. The tryptic-like site displays a large unstructured S1 specificity pocket,[50] allowing for motion and flexibility of the P1 leucine side chain of the bound ligand. Although bortezomib adopts a β-conformation in the tryptic-like active site, similar to what has been observed for subunits β1 and β5, its P1 leucine side chain does not form hydrophobic interactions with residues of the S1 specificity pocket, thus destabilizing the complex at this site. As already discussed, the probability of covalent binding of bortezomib to various proteolytically active site threonine residues correlates well with the residence time of the inhibitor at the active centers, which, in turn, depends on the affinities of the ligand for the individual binding clefts. Low binding affinity of the boronic P1 leucine side chain to the S1 pocket may lead to a reduced occupancy of bortezomib in the tryptic-like active site, thus increasing its IC_{50} value, which is in accord with functional results obtained *in vivo*.[134]

The binding mode of the P2 phenylalanine side chain of bortezomib to the proteasomal S2 pockets revealed some unexpected structural results. Since proteasomes exhibit no specific S2 pockets, all active sites are able to generally accept space demanding side chain residues.[45] However, crystallographic data of the proteasome−bortezomib crystal structure showed that the conformation of the P2 phenylalanine side chain of bortezomib is flipped in the tryptic-like active site, compared to its conformation in the chymotryptic and caspase-like activity. This result is a surprise, since both conformations of the P2 phenylalanine side chain of bortezomib would fit in the three distinct specificity pockets of the various proteolytically active sites, without making contact with protein residues. Thus, the P2 site of bortezomib possibly contributes to the overall pharmacodynamic properties but surely not to the kinetics of inhibition. Presumably, a specific gain may be obtained by the introduction of large hydrophobic moieties at the P2 site.[112,113,145−147]

The binding probabilities of bortezomib by the P3 pyrazyl group revealed some interesting insights for the ligand stabilization, since specific interactions are formed between the ligand and protein residues of the subunit specific S3 pockets. In the case of the chymotryptic-like active site, the P3 pyrazyl ring is hydrogen bridged to the hydroxyl group of Asp114 of the adjacent β6 subunit. Only one of the nitrogen atoms of the pyrazyl residue is stabilized, but the observed interaction is strong, as evidenced by the short bond length of 2.9 Å. The experimental electron density reveals a well-defined water molecule in proximity to Asp114O$^{\gamma}$, which coordinates a tight hydrogen-bonding network, performing interactions with β6Asp114O$^{\gamma}$, β5Ala49N, and β5Ala50N of the protein and with the carbonyl oxygen of bortezomib (Figure 6b2). In the case of the caspase-like activity, the pyrazyl side chain is only hydrogen bridged to Thr22O$^{\gamma}$ of subunit β1 (2.9 Å). Position 114 of the neighboring subunit β2 displays a histidine residue, which does not interact with the pyrazyl ring. Therefore, only the carbonyl oxygen of β1Ala40 stabilizes the peptide backbone of bortezomib by formation of the β-conformation, whereas a defined water molecule, present in the chymotryptic-like active site, is absent in the caspase-like active site. Important interactions of the pyrazyl ring of β2-bound bortezomib are lacking in the tryptic-like active site. Though an aspartic residue is present at position 114 of the adjacent subunit β3 with similar orientations as described for the chymotryptic-like active site, the S3 binding pockets of these two proteolytically active sites differ significantly, thus providing further explanation for the subunit selectivity of bortezomib. Upon closer inspection of the pyrazyl moiety, it becomes evident also that the P3 site is critical for the high affinity of bortezomib for the chymotryptic-like active site. Thus, alterations of the P1 and P3 sites may significantly improve the binding properties of the inhibitor to the respective proteolytically active sites.

4.4.4. Biological Significance and Structure-Based Improvement of Bortezomib

The clinical use of bortezomib makes it imperative that its binding mode to mammalian proteasomes is clarified, not only to fully understand the mechanism of inhibition but also to provide a platform for rational improvements of specificity and strength of inhibition. The structural superposition of bovine liver[51] and yeast[50] proteasomes shows the expected high degree of structural similarity.The ability of bortezomib to inhibit individual subunits of the yeast proteasome conforms to kinetic data obtained for mammalian proteasomes.[134,148] This is shown by independent measurements of the catalytic activities of the yeast proteasome upon treatment with bortezomib as recorded by the use of fluorogenic substrates in the absence of sodium dodecylsulfate or activators.[140] So far, biochemical and crystallographic characterization of active site mutants has been performed only in yeast[65,75,80] and mutagenic inactivation of proteasomal active site residues has revealed some striking phenotypes. In particular, the Thr1:Ala mutation of the active site subunit β5 is lethal and the Lys33:Ala mutation causes severe growth defects, whereas the β1Thr1:Ala and β2Thr1:Ala active site mutations are less toxic. It is, therefore, important to understand the physiological contributions of single proteasomal subunits in the mammalian system, which can be addressed by specific, subunit selective, and cell permeable proteasome inhibitors. The crystal structure of bortezomib bound to the yeast proteasome illustrates concerted movements that affect the binding affinities of the inhibitor to the proteolytic active sites. Since bortezomib is now used for the treatment of the lethal hematologic malignancy multiple myeloma, with clinical trials for other malignancies ongoing, it is important to understand its mode of action at the molecular level. The structural data for the bortezomib−proteasome complex explain the different *in vivo* binding affinities of the ligand for the individual subunits at atomic resolution. These data also propose new possibilities for the design of bortezomib derivatives with superior inhibition characteristics and for the design of inhibitors that will specifically bind to single proteolytically active sites.

4.5. Peptide Epoxyketones

In the search for antitumor agents displaying specific activity against B16 murine melanoma, natural peptidyl α',β'-epoxyketones were discovered: eponomycin from *Streptomyces hygroscopicus*[149,150] and epoxomicin from the actinomycete strain Q996-17.[151] Using biotinylated epoxomicin as a molecular probe,[152] it was shown that peptidyl α',β'-epoxyketones covalently bind to the proteolytically active subunits of the proteasome,[153] consequently inhibiting their activity. First, enzymatic assays with epoxomicin and purified bovine erythrocyte proteasome revealed that this compound primarily affects the chymotryptic-like activity.[145] The tryptic- and caspase-like activities are inhibited at 100- and 1000-fold slower rates, respectively.[154] Unlike most other proteasome inhibitors, epoxomicin is highly specific for the proteasome and does not inhibit other proteases such as calpain, trypsin, chymotrypsin, papain, or cathepsins.[155] The crystal structure of the yeast 20S proteasome in complex with epoxomicin clarified this unique specificity of α',β'-epoxyketones for proteasomes.[156] Comparison of the crystal structure of the proteasome complexed with calpain inhibitor I^{50} with the proteasome−epoxomicin structure reveals that both the peptide aldehyde and epoxomicin bind similarly to the catalytic subunits, completing an antiparallel β-sheet. However, a striking difference was obvious in the formation of the covalent adduct formed by each inhibitor with the amino terminal Thr1. Whereas the peptide aldehyde forms a hemiacetal bond with the Thr1O$^{\gamma}$, a well-defined electron density map of epoxomicin at the active site reveals the presence of a unique six-membered morpholino ring system (Figure 6c1). This morpholino derivative results from adduct formation between the α',β'-epoxyketone pharmacophore of

epoxomicin and the amino terminal active site nucleophile Thr1O$^{\gamma}$ and N. The formation of the morpholino ring is apparently a two-step process: first, activation of the Thr1O$^{\gamma}$ occurs by its N-terminal amino group directly or via a neighboring water molecule acting as the base. Subsequent nucleophilic attack of Thr1O$^{\gamma}$ on the carbonyl carbon atom of the epoxyketone pharmacophore produces a hemiacetal, as observed in the structure of proteasome−aldehyde inhibitor complexes. This hemiacetal bond facilitates the second step in the formation of the morpholino adduct. In this intramolecular cyclization, Thr1N opens the epoxide ring via an intramolecular displacement with consequent inversion of the C2 carbon. The nucleophilic attack by Thr1N occurs at C2 and not at the neighboring, less hindered C1 methylene of the epoxide (Figure 6c2). Thus, the resulting morpholino adduction formation is the favored 6 *Exo-Tet* ring closure[157] instead of the 7 *Endo-Tet* ring closure, which would result from attack at the less hindered C1 epoxy methylene. Further experimental evidence for the presence of a morpholino adduct at the active site of the proteasome comes from mass spectrometric analysis, which was performed after HPLC separation of the epoxomicin-bound catalytic subunits under acidic conditions, when the hemiacetal bond of the morpholino ring is opened. The observed masses of the subunits confirmed the irreversible covalent binding of epoxomicin.[129] A major significance of the morpholino adduct that results from epoxomicin binding to the proteasome is that it provides the structural basis for epoxomicin's unique specificity for the proteasome. Since other proteases, which are common targets for many proteasome inhibitors such as peptide aldehydes, vinyl sulfones, and boronic acids, do not have an amino terminal nucleophilic residue as part of their active sites, epoxomicin cannot form the same morpholino adduct with these proteases as it does with the proteasome. Thus, the observed selectivity of epoxomicin for proteasomes is rationalized by the requirement for both an N-terminal amino group and a side chain nucleophile for adduct formation with the epoxyketone pharmacophore. Members of the N-terminal nucleophilic family of hydrolases also possess an amino terminal amino acid with a nucleophilic side chain. However, it still has to be tested whether epoxyketones can act as a general pharmacophore for this small hydrolase family. An interesting observation was made when the proteasome inhibitory activities of the two C2 epimers of epoxomicin were compared. While the naturally occurring (*R*) C-2 isomer potently inhibits proteasome activity, the 2(*S*) C-2 epimer is more than 100-fold less potent .[152]

Proteasome inhibition is being extensively evaluated for a variety of therapeutic purposes, and the need for potent and selective small molecule proteasome inhibitors is well recognized. Recently, other linear α′,β′-epoxyketone natural products from *Streptomyces sp.*, TMC-86,[158] TMC-89,[159] and TMC-96[160] have been isolated during screening of proteasome inhibition by the components from microbial metabolites. Additionally, further peptide epoxyketone proteasome inhibitors have been synthesized, such as YU101, which displays specificity for each of the three proteolytic activities of the proteasome.[145] The unique binding mechanism of epoxyketones makes them one of the most selective inhibitors: it was shown that proteasomal subunits are the only cellular proteins covalently modified by biotinylated derivatives of epoxomicin and eponemycin.[153,155] However, the possibility that epoxyketones may reversibly inhibit other enzymes has not been studied so far.

4.6. β-Lactones

4.6.1. Lactacystin

Lactacystin, a natural compound produced by *Streptomyces sp.*, was the first identified natural proteasome inhibitor originally discovered as an inducer of neuritogenesis in neuroblastoma cell lines.[161−167] Radioactive lactacystin was shown to bind mainly to the proteasomal subunit β5,[166] effectively and irreversibly inhibiting the chymotryptic-like activity. The tryptic-like and the caspase-like activities are also blocked, but to a lower extent.[168] Surprisingly, subsequent *in vitro* studies demonstrated that lactacystin itself is not active against proteasomes. Further investigations showed that in aqueous solutions at pH 8 the reactive compound of lactacystin is spontaneously hydrolyzed into *clasto*-lactacystin β-lactone,[169] also termed omuralide,[170] which acts as the functional reactive group (Figure 7a1). The crystal structure analysis of the yeast proteasome−omuralide complex[50] confirmed previous functional studies: the structure shows that omuralide is covalently bound only to subunit β5, which is in line with the observed chemical modification of subunit β5/β5i of mammalian proteasomes (Figure 7b1).[166] Furthermore, the nucleophilic water molecule, which hydrolyzes the acyl ester intermediate to release the peptide and to restore the active site Thr1O$^{\gamma}$ of the enzyme, is structurally distorted.[50,140] The data suggest the following mechanism of the inhibition reaction: after cleavage of the β-lactone, the generated hydroxy group C3-OH of the inhibitor occupies the position formerly taken by a well-defined water molecule in the unligated form.[70] The γ-lactam ring in lactacystin prevents free rotation around the C-3/C-4 bond, helping to maintain C3-OH in this position (Figure 7c). As the preferred trajectory of nucleophilic addition is along the path approximately perpendicular to the plane of the ester group,[74,171] the two possible faces of attack on Thr1O$^{\gamma}$-CO by water are blocked either by protein residues or by the generated C3-OH ligand hydroxy group, resulting in inefficient deacylation of the Thr1O$^{\gamma}$. Besides the covalent acyl ester bond, omuralide is bound to proteasome main chain atoms by a large number of hydrogen bonds. However, the main reason for increased selectivity of this inhibitor for the chymotryptic-like active site is the apolar nature of this site's S1 specificity pocket. Omuralide contains a less reactive head group and, therefore, needs longer time to react with the Thr1O$^{\gamma}$ than calpain inhibitor I. Therefore, the neutral charge pattern of the S1 pocket of the chymotryptic-like activity is important for prolongation of the mean residence time of the inhibitor at the active site, for completion of the covalent binding to the active residue. The neutral character of the S1 specificity pocket is mainly provided by Met45 of subunit β5, and the inhibitor can be stabilized only at this site, with its dimethyl side chain being sufficiently long to complete the ester bond formation between the *clasto*-lactacystin β-lactone and Thr1O$^{\gamma}$. These observations indicate that both the functional head group and side chain residues of ligands play a significant role in their selective and specific binding to single proteolytically active subunits of the proteasome.

4.6.2. Salinosporamide A

Salinosporamide A, a small secondary metabolite of the marine actinomycete *Salinispora tropica*,[172,173] is a highly potent and selective inhibitor of the proteasome, currently undergoing clinical studies as potential drug for cancer treatment.[174] Though structurally related to omuralide,[162]

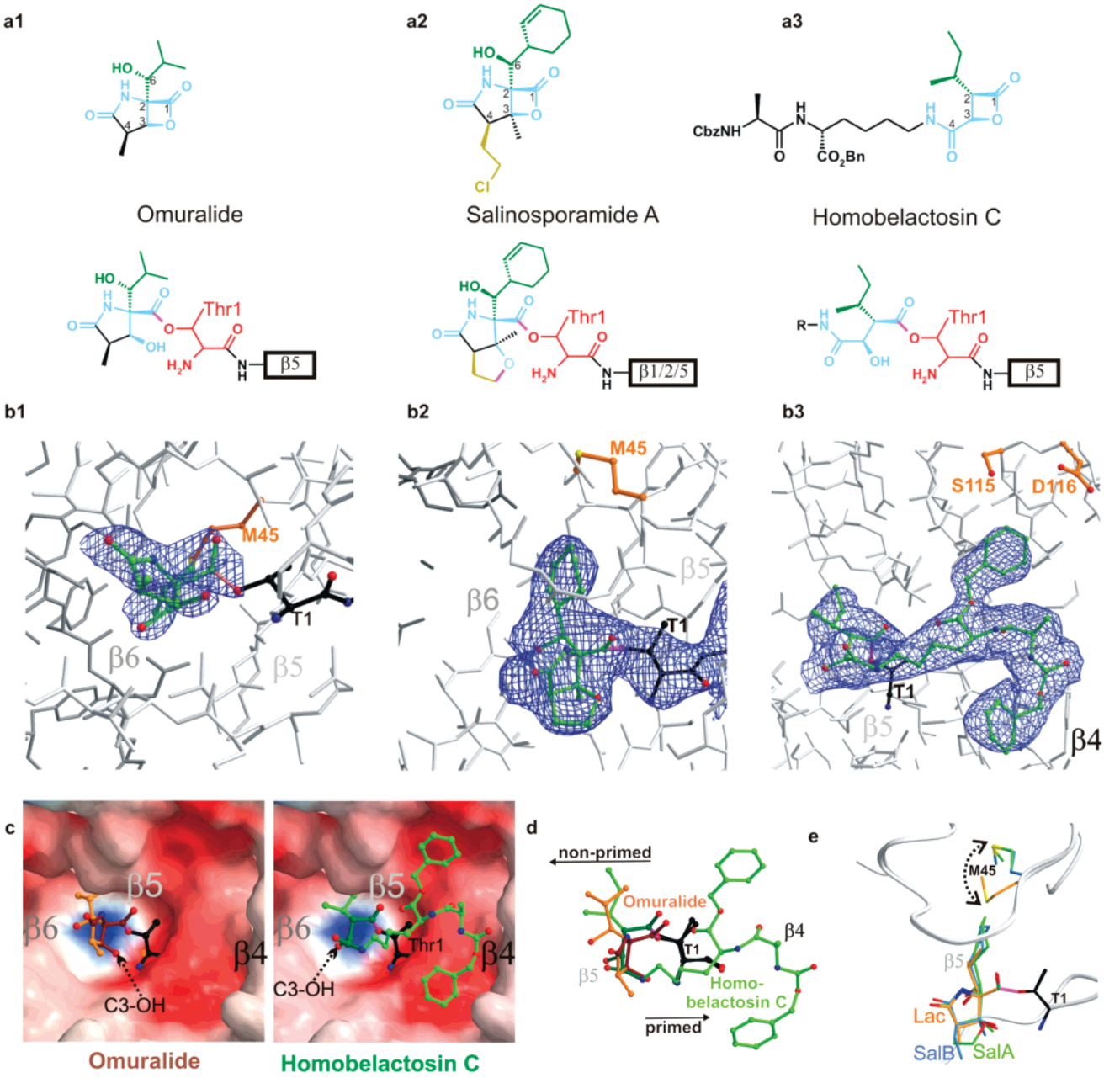

Figure 7. Inhibition of proteasomal active sites by β-lactones with formation of covalent acyl ester bonds. (a1−a3**)** Chemical structures of omuralide, salinosporamide A, and bis-benzyl-protected homobelactosin C in their native and bound conformations. The lead structure segments which in particular are involved in inhibitor binding are depicted in blue; Thr1 of subunit β5 is depicted in red. Active sites of the yeast proteasome in complex with (b1**)** omuralide,[50] (b2**)** salinosporamide A,[70] or (b3**)** bis-benzyl-protected homobelactosin C.[94] All inhibitors follow a common binding mechanism. Residues which are characteristic for ligand specificities (Met45 in the case of omuralide and salinosporamide A; Ser115 and Asp116 in the case of homobelactosin C) are orange. (c**)** Surface representation of the chymotryptic-like active site in complex with omuralide (depicted in brown, left panel) and homobelactosin C (depicted in green, right panel), covalently bound to Thr1 (depicted in black). Note the overall similarity in the binding mode of both inhibitors but the different orientations of the generated C3-hydroxy group upon β-lactone ring opening (indicated by a black arrow). (d**)** Superposition of omuralide and bis-benzyl-protected homobelactosin C including Thr1 of subunit β5. Omuralide is shown in brown, bis-benzyl-protected homobelactosin C is drawn in green, and the active site Thr1 is shown in black. The superposition indicates that all inhibitors occupy the S1 specificity pocket similarly; however, only the bis-benzyl-protected homobelactosin C is prolonged to the primed site. Nonprimed and primed sites are indicated by a black arrow. (e**)** Role of Met45 of subunit β5 in the formation of the S1 specificity pocket. Met45 tightly interacts with the branched side chain of omuralide and salinosporamides. In the case of omuralide-binding, Met45 minimizes the size of the S1 pocket, whereas Met45 is rearranged by 2.7 Å in the proteasome−salinosporamide complexes, thus performing for each ligand optimal interactions.

salinosporamide A contains several unique substituents, including a cyclohexene ring in place of the isopropyl group, and a chloroethyl group in place of the methyl group (Figure 7a2), that collectively enhance its potency both *in vitro* and *in vivo*.[175] Remarkably, in contrast to omuralide, which exists in nature in the form of its precursor thioester lactacystin, thioesters of salinosporamide A have not been found in nature but have been made semisynthetically.[253] Such forms of the molecule would give rise to chlorine elimination, prematurely releasing the trigger of the chemical reaction (see below). Given the structural similarities between omuralide and salinosporamide A, the covalent acyl ester binding of this inhibitor to the proteasomal active site could be expected, which was confirmed by crystal structure analysis. However,

the structural data revealed that, in contrast to omuralide, salinosporamide A was bound to all six catalytic subunits. Furthermore, the structure provided explanations for the enhanced potency of salinospramide A compared to omuralide:[70] the generated C3-O group of salinosporamid A subsequently forms a cyclic tetrahydrofuran (THF) ring with the chloroethyl side chain, causing an enthalpically and entropically favorable binding mechanism associated with the release of HCl. These findings support the existence of a two-step binding mechanism in which addition of Thr1O$^{\gamma}$ to the β-lactone carbonyl is followed by nucleophilic addition of C3-O to the chloroethyl group, giving rise to the cyclic ether (Figure 7b2).[70,175] Thr1O$^{\gamma}$ is similarly acylated by the inhibitor, as has been described for the peptide substrate, and might similarly occur through a tetrahedral intermediate. Cleavage of the acyl ester intermediate by the nucleophilic water molecule is challenged by the spacial arrangement of C3-O of the inhibitor at the active site. The N-terminus is positioned for hydrogen bonding with the inhibitor C3-OH. In the case of salinosporamide A, chlorine is eliminated and the N-terminus is fully protonated.[70] These findings prove the earlier hypothesis about Lys33 not being the proton acceptor and, therefore, having an impact on the intrinsic pK_a of both Thr1O$^{\gamma}$ and Thr1N[50] (see also section 3.2).

On the basis of the chemical structure of salinosporamide A, a new compound with the chlorine atom at the ethyl-C2 substituent replaced by a hydrogen atom was found (salinosporamide B, a natural compound from *Salinispora tropica*[175,176]). Crystal structure analysis of the proteasome in complex with this new inhibitor revealed that the unreactive ethyl substituent in salinosporamide B circumvents formation of the THF ring.[70] Since in proteasomes P2 side chains of ligands are not bound to the protein, there is sufficient space to accommodate a methyl group (omuralide), an ethyl group (salinosporamide B), a THF ring (salinosporamide A), and, most likely, also larger side chains. Some examples of these chemical modifications have been reported previously.[175] Further comparison to omuralide shows differences in the P1 site of salinosporamide A, which is increased from an isopropyl group to a cyclohexenyl ring. These substituents interact with Met45 of the β5 S1 binding pocket, which is involved in key enzyme−substrate interactions during hydrolysis of peptide bonds containing hydrophobic amino acids (chymotryptic-like activity). In order to accommodate the larger cyclohexenyl ring of salinosporamide A, Met45 structurally rearranges similarly as has already been described for the proteasome−calpain inhibitor I complex (Figure 7e). Although the flexibility of side chains in proteins makes it difficult to predict optimal substitution at this site, the structural data indicate that additional hydrophobic interactions exist between atoms of the cyclohexene ring and residues of the S1 pocket for subunit β5, thus explaining the enhanced potency of salinosporamide A as compared to omuralide.

4.6.3. Belactosines

Belactosin A and C, natural products from *Streptomyces* sp. UCK14, exhibit antitumor activity,[177,178] which has been shown to be significantly increased upon acetylation of the free amino group and esterification of the carboxyl group, as well as replacement of the ornithine moiety with lysine to furnish bis-benzyl-protected homobelactosin A and C (Figure 7a3).[179,180] The latter shows IC_{50} values against human pancreoma and colon cancer cells at the low nanomolar level.[181] The high antitumor activity of these compounds has been attributed to inhibition of the proteasomal activity.[181] The crystal structure analysis of the yeast proteasome in complex with bis-benzyl-protected homobelactosin C reveals specific acylation of the free hydroxy group of the N-terminal Thr1O$^{\gamma}$ of the chymotryptic-like active site (Figure 7b3),[94] in close analogy to what has been observed for omuralide[50] and salinosporamides.[70] However, although omuralide, salinosporamide A and B, as well as homobelactosin C are identically linked to the Thr1O$^{\gamma}$, homobelactosin C follows a unique mechanism to prevent cleavage of its newly formed ester bond. As previously described for omuralide, the generated C3-OH group occupies the position formerly taken by the nucleophilc water molecule, thus preventing deacylation. The presence of the γ-lactam ring in omuralide prevents free rotation about the C-3/C-4 bond, and the newly generated hydroxy group at C3 forms a hydrogen bond to the amino group of Thr1 (Figure 7c). In contrast, the generated hydroxy group at C3 of bis-protected homobelactosin C points into the opposite direction and forms a hydrogen bond to Arg19O with a distance of 2.7 Å. A similar role is fulfilled by C6-OH of omuralide and salinosporamides. The amide nitrogen of the 3-aminocarbonyl side chain of bis-benzyl-protected homobelactosin C adopts a similar position to that of the C3-OH of omuralide and salinosporamide, and the remainder of the side chain is bound to the primed site of the proteasome (Figure 7d).[50,70,94] Omuralide has been found to specifically block the chymotryptic-like active site, since the unique neutral charge pattern of the S1 pocket at this site stabilizes the ligand for completion of the ester bond formation between the *clasto*-lactacystin β-lactone and Thr1O$^{\gamma}$. The structural superposition of bound omuralide and homobelactosin C shows a remarkable overlap of their P1 residues. However, homobelactosin C additionally contains the sterically demanding 3-aminocarbonyl side chain, which only fits to the primed chymotryptic-like active site, as it would cause a steric clash with residues of the caspase- and tryptic-like active sites. It was shown that the benzyl ester derivative of belactosin A (IC_{50} = 48nM) is 5 times more potent than belactosin A itself .[181] The homobelactosin C derivative described here contains the same protective groups. The crystallographic data reveal characteristic hydrophobic interactions of the benzyl groups with protein residues, which offer a rational explanation of the observed IC_{50} values. Since the primed specificity pocket is also negatively charged, in particular by β5-Asp114 and β5-Asp116 moieties, appropriate positively charged substituents may further decrease the IC_{50} value of the homobelactosin C derivative (Figure 7c). The 3-aminocarbonyl side chain of bis-protected homobelactosin C cannot be directly compared to protein substrates, since proteins can use many residues or side group elements for further stabilization. Nevertheless, the binding mode of the homobelactosin C derivative for the first time indicates the preferred trajectory of ligand and substrate binding to the primed site of the proteasome.[94] It was shown that, though human constitutive subunit β5 and immuno subunit β5i share extensive sequence homology, they significantly differ in the nature of produced peptides.[182] Comparison of the primary sequences of subunits β5 and β5i shows a significant difference in residues which closely interact with the benzyl side chain of the bis-protected homobelactosin C. This information may serve as a guide for design and synthesis of new compounds, specific for proteasomal constitutive or immuno subunits (see also section 3.5).

4.7. Noncovalent Proteasome Inhibitors: TMC-95 and Its Derivatives

All of the previously described proteasome inhibitors form a covalent bond with the active site Thr1O$^{\gamma}$ of the β-subunits. Application of these inhibitors *in vivo* often induces apoptosis and causes cell death.[167,183,184] It can be expected that the cytotoxic effects of proteasomal inhibitors may be reduced by making their binding to proteasomes reversible and time-limited. Recently, it was shown that the natural products from *Apiospora montagnei*, TMC-95s (TMC-95A, B, C, and D), selectively and competitively block the proteolytic activity of the proteasome in the low nanomolar range.[185,186] Furthermore, it was reported that TMC-95-compounds do not inhibit other proteases such as m-calpain, cathepsin L, and trypsin.[185] TMC-95 compounds, which are not related to any previously mentioned proteasome inhibitors, consist of a heterocyclic ring system made of modified amino acids (Figure 8a1). The inhibitor binds to all three proteolytically active sites, as was elucidated from the crystal structure of the yeast proteasome in complex with TMC-95A.[156] TMC-95A is linked noncovalently to all proteolytically active β-subunits, not modifying their N-terminal threonines. A tight network of hydrogen bonds connects TMC-95A with the protein, thus stabilizing its position. All these interactions are performed with main chain atoms and strictly conserved residues of the proteasome, revealing a common mode of proteasome inhibition among different species. The arrangement of TMC-95A in the proteasome is similar to that of the already described aldehyde and epoxyketone inhibitors.[81] The n-propylene group of TMC-95A protrudes into the S1 pocket, making weak hydrophobic contacts with the hydrophobic part of Lys33, whereas the shallow S2 subsite does not contribute to stabilization of the inhibitor. TMC-95A was described to block the distinct proteolytically active sites with different IC_{50} values.[185] This fact can be structurally explained by the presence of the asparagine side chain at the P3 site, which is in close contact with the distinct S3 pockets. Furthermore, this observation is in line with results obtained for aldehyde[115] or vinyl sulfone inhibitors,[130] which changed their binding efficiencies by modifications only in their P3 and P4 sites. It was reported that the IC_{50} values for the stereoisomers of TMC-95s vary by 2 orders of magnitude.[185] The structural data of the proteasome−TMC95A complex revealed that for effective ligand binding the hydroxy group in position C7 of the TMC-95s must be in its S-isomeric state, in order to avoid a steric clash with the carbonyl oxygen of residue 21, whereas the methyl group in position C36 is not sterically restricted (Figure 8a1). These results confirm once again that the prerequisite for selective and efficient inhibitor binding is the topology of proteasomal active sites and not proteolytically active residues.

Analysis of the crystal structure of the proteasome−TMC-95 complex has revealed which residues of TMC-95s are essential for binding.[156] Superposition of the crystal structure of TMC-95A with the NMR structure of unbound TMC-95A in solution[186] showed no conformational rearrangements of the inhibitor upon binding to the proteasome.[156] Thus, optimal binding of this inhibitor to the proteasome is due to the strained conformation of TMC-95s, caused by the presence of the cross-link between the tyrosine and the oxoindol side chain. Binding of TMC-95s does not require major rearrangements of residues of ligand and protein and, therefore, is entropically favored, in contrast to more flexible ligands. The structural superposition of proteasomal subunits in complex with TMC-95A and Ac-PRLN-vs shows a remarkable overlap of the backbone amides and the P1 and P3 residues, although TMC-95A binds noncovalently and Ac-PRLN-vs binds covalently to the active Thr1O$^{\gamma}$. This observation demonstrates that if specific ligands of the inhibitor are presented in an optimal manner, covalent attachment to the catalytic nucleophile is no longer required. Having a basic inhibitor structure with the geometry of TMC-95s, a variety of compounds specific for each proteasomal active site could be created by combining information obtained from various crystal structures of proteasome−inhibitor complexes. In particular, the P1 and P3 sites are the basis for fine-tuning of the inhibitor's selectivity for individual β-subunits.

4.8. Endocyclic Oxindol-Phenyl-Bridged Tripeptides

Proteasome inhibition has promising therapeutic potential. That is why much attention has been paid to the development of synthetic ligands modulating the activity of the proteasome. The natural proteasomal inhibitor TMC-95A has proved to be an effective and a reversible compound. TMC-95A binds to the specificity pockets of proteasomal active sites mainly by formation of hydrogen bonds between its rigid extended peptide backbone and the protein, with creation of an antiparallel β-sheet structure (Figure 8c1). As has been seen in the crystal structure, the tyrosine residue of TMC-95A interacts only weakly with the shallow hydrophobic S4 subsites of all active sites, while the hydroxy group is exposed to the solvent. Similarly, the N-terminal 3-methyl-2-oxopentanoyl group is exposed to the bulk solvent without apparent interactions with the protein. Thus, the conformationally restricted C-terminal (*Z*)-prop-1-enyl moiety as a P1 residue and the central asparagine as a P3 residue are mainly responsible for the differentiated binding affinities of TMC-95A to the three active sites. However, the total synthesis of the TMC-95A is highly complex and appears not to be feasible.[187−190] Using information obtained from the crystal structure of the TMC-95A−proteasome complex,[156] a minimal TMC-95 core structure was derived (Figure 8a2).[188] The new lead was used to create a number of more synthetically feasible TMC-95A analogues, as well as for investigations of the relative energetic contributions of the single chemical bonds of the ligand to the differentiated inhibitory potencies of TMC-95A against the β1, β2, and β5 proteolytic activities.

First, the minimal TMC-95 core was decorated C-terminally with an *n*-propyl group as a P1 residue and N-terminally with benzyloxycarbonyl as an N-protecting group, while the central Asn residue of TMC-95A was retained as a P3 residue (TMC-95-2a).[191] The crystallographic analysis of the proteasome complexed with this TMC-95-2a analogue revealed the formation of the same hydrogen-bonding network as has been observed for TMC-95A. However, TMC-95-2a shows a strongly differentiated binding affinity for the three distinct active sites as compared to the case of TMC-95A. Replacement of the P1 residue of TMC-95A with the flexible *n*-propyl chain leads to decreased binding affinities for all three active sites by at least 1 order of magnitude.[189] It is a well-established fact that efficient occupation of binding pockets by shape- and charge-complementary ligand moieties is defining the affinities of the inhibitor molecules for the active sites.

Further, a second TMC-95-2b analogue was designed in which the (*Z*)-prop-1-enyl group of TMC-95A was replaced

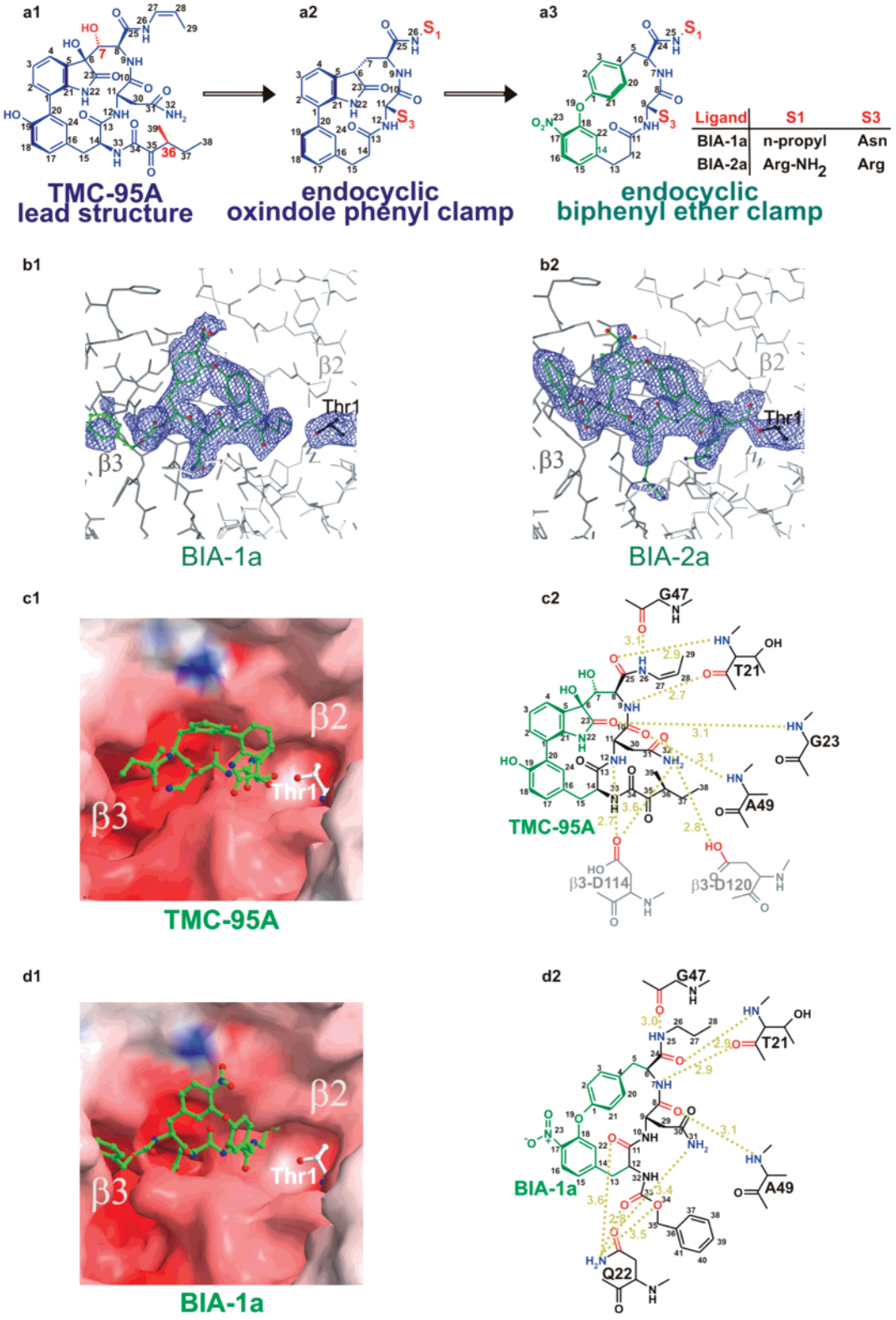

Figure 8. Reversible inhibitors of the proteasome. (a**)** Chemical structure of the lead component of TMC-95A (a1) and structurally derived endocyclic oxindole-phenyl compounds (a2).[156,188,191] The endocyclic biphenyl ether clamp (a3), colored in green, restricts conformationally the tripeptide derivatives and, thus, preorganizes the peptide backbone for its high affinity binding to the proteasomal active site clefts. S1 and S3 specificity sites are the major determinants for differential binding of the inhibitor to various active proteasomal subunits.[193,197] (b1−b2**)** Representation of the tryptic-like active site of the yeast 20S proteasome (subunits $\beta 2$ and $\beta 3$ are white and gray, respectively) in complex with BIA-1a and BIA-2a. The covalent linkage of BIA-2a to subunit $\beta 2$ Thr1O$^{\gamma}$ is drawn in magenta. Electron density maps of the bound inhibitors are blue. (c1−c2 and d1−d2) Flexibility of the S1 binding pocket of the proteasomal tryptic-like active site. Surface representation of (c1**)** TMC-95A and (d1**)** BIA-1a bound to the proteasomal tryptic-like active site. Thr1, shown in white, is not linked to these ligands. Surface colors indicate positive and negative electrostatic potentials. Note the different conformations of proteasomal side chain residues upon TMC-95A and BIA-1a binding. Schematic representation of TMC-95A (c2) and BIA-1a (d2) bound to the proteasome. Hydrogen bonds are illustrated as yellow dashed lines. Distances are shown in angstroms. Residues of subunits which are involved in specific ligand interactions are shown in black (subunit $\beta 2$) and gray (subunit $\beta 3$).

by a norleucine side chain and aspargine was replaced by leucine for a possible change in the selectivity pattern, thus generating an inhibitor with higher specificity for the chymotryptic-like activity of the proteasome. In the case of calpain inhibitor I[50] and peptide vinyl sulfones,[130] similar P1 and P3 residues were found to be efficient for enhancing specific inhibition of the chymotryptic-like activity. Moreover, the superposition of the crystal structures of those inhibitors in complex with the proteasome with that of TMC-95A showed an almost identical peptide backbone display, thus suggesting that leucine and norleucine side chains will adopt the orientations when incorporated into TMC-95A as P1 and P3 residues, respectively. Larger size P1 residues had been shown to induce structural rearrangements of β5-Met45 of the chymotryptic-like S1 pocket.[50] However, in the case of TMC-95-2b, which has the norleucine side chain in P1, Met45 did not rearrange and, in order to prevent a steric clash in the S1 pocket, the norleucine side chain pushes the peptide backbone of the biaryl group apart from the optimal binding position in the active site cleft. This provides the basis for the lower binding affinity of TMC-95-2b: its IC_{50} value is increased 100-fold compared to that of TMC-95A.[191] Since the tryptic-like active site contains a spacious S1 pocket, the structural arrangements and inhibition rates of TMC-95-2b and TMC-95-2a are similar, whereas TMC-95-2b does not bind to the caspase-like active site due to its small and positively charged S1 pocket.

4.9. Endocyclic Biphenyl Ether-Bridged Tripeptides

As previously discussed, the constrained conformation of the TMC-95 class of inhibitors provided the basis for creation of compounds with entropically enhanced binding affinity. Since synthesis of TMC-95A is a complex task,[188−190,192] attempts have been undertaken to take advantage of the rigidity of this unique molecule in the design of synthetically less demanding reversible inhibitors of the proteasome. Comparison of the conformational preferences of TMC-95s and their derivatives in solution and in proteasome bound states revealed that the lower inhibitory potencies could only derive from the conformational flexibility of groups mimicking the P1 residue. This observation allowed creation of a more flexible endocyclic clamp, in particular the biphenyl ether group of the isodityrosine type,[193] which is known to preorganize the peptide backbone in a rigidly extended conformation (Figure 8a3).[194−196] The biphenyl ether BIA-1a, having an *N*-propyl group at P1 and an Asn residue at P3, was designed in order to compare endocyclic oxindolphenyl-bridged and endocyclic biphenyl-ether-bridged tripeptides structurally and functionally. The kinetic assays revealed that BIA-1a has approximately 2-fold lower proteasomal inhibition activity as compared to TMC-95A.[193] Surprisingly, the crystal structure analysis of BIA-1a in complex with the proteasome showed that the ligand was only bound to the tryptic-like active site, in proximity of Thr1O$^{\gamma}$ of subunit β2 (Figure 8b1).[197] This exclusive binding of BIA-1a was explained by the unique architecture of the specificity pockets of the tryptic-like active site. A comparison of crystal structures of the proteasome in complex with TMC-95A and with BIA-1a revealed that TMC-95A and its biphenyl ether derivative follow a unique binding conformation (Figure 8d1). However, the structural superposition of both ligands bound to the tryptic-like active site also showed a striking difference: though BIA-1a and TMC-95A have a high degree of consensus in their constrained geometry, conformation, and binding mode, TMC-95A is additionally hydrogen bridged by the CO of the oxindole to the NH of Gly23 (Figure 8c2). Since this functional group is absent in the endocyclic biphenyl ether of BIA-1a, its extended β-type backbone conformation is destabilized, as compared to that of TMC-95A. Moreover, it is the strong interaction of BIA-1a with residues exclusively found in the tryptic-like active site formed by subunits β2 and β3 which explains its high selectivity (Figure 8d2). As expected, the conformation of BIA-1a in solution as determined by NMR[193] does not change in a detectable manner upon its binding to the active site of the proteasome, demonstrating the efficiency of the endocyclic biphenyl ether clamp for conformational preorganization of the ligand backbone for optimal binding to the active site cleft.

The structural information derived from the proteasome−BIA-1a complex provided the basis for the design of an advanced β2-selective compound for inhibition of the tryptic-like proteasomal activity. A selective inhibition of subunit β2 was achieved with the synthetic peptidyl-vinylsulfone Ac-PRLN-VS derivative, while its analogue Ac-YLLN-VS showed nonspecific binding to all active centers.[112,130] This result suggested that inhibitor selectivity is dependent on the S1 as well as the S3 pocket. Knowing that the S1 pocket of β2 subunits is particularly compatible with basic residues,[115] a modified endocyclic biphenyl ether compound BIA-2a with Arg side chains in both the P1 and P3 positions was designed and synthesized (Figure 8a3). Furthermore, the C-terminus of BIA-2a was extended by an amide group to achieve close contact with Thr1O$^{\gamma}$.[193] The crystallographic data of BIA-2a in complex with the proteasome revealed formation of a covalent ester bond between BIA-2a and the Thr1O$^{\gamma}$, i.e. formation of the acyl enzyme intermediate as the first step in amide hydrolysis (Figure 8b2).[197] Indeed, mass spectrometric analysis of yeast proteasome incubated with BIA-2a confirmed hydrolysis of the C-terminal amide within 2 h at room temperature. These findings confirmed that the proteasomal proteolytically active sites maintain their functional efficiency upon binding of the inhibitor BIA-2a. The overall binding mode of BIA-2a is similar to that of BIA-1a, with almost identical backbone geometry. Therefore, TMC95-A and its biphenyl ether derivatives bind to the proteasomal active sites noncovalently in a reversible substrate-like manner, causing no allosteric changes of the active site residues.[197] Covalent derivatization of the active site Thr1O$^{\gamma}$ and its subsequent deactivation is a central feature of all irreversible inhibitors which form an ester bond with active site threonine, including the small-size lactacystin, salinosporamide A, and homobelactosin C.[50,70,94] The slow rate of hydrolysis of these inhibitors can be explained by the out-of-place positioning of the nucleophilic water molecule upon inhibitor binding. However, this hypothesis could not be proved experimentally, since the exact localization of this water molecule in the proteasome−BIA-2a complex was not clear due to insufficient electron density at this position.[197] Nevertheless, the clearly visible ester bond as an intermediate step of amide hydrolysis of BIA-2a confirms that the half-lives of intermediate complexes of the proteasome with tight-binding substrates could well suffice for rates of aminolysis that compete with hydrolysis. To analyze, whether such reversed proteolysis can indeed occur in the cavity of the proteasome, yeast proteasome was incubated with BIA-2a and an excess of H-Ala-Gly-OH. Mass spectrometric analysis

of the incubation medium failed to detect spliced C-terminally extended BIA-2a species by the dipeptide amide,[197] which is in agreement with experiments, showing that proteasomal degradation products are obtained from substrate specific cleavage patterns.[76] Furthermore, these results confirm experiments reported by Vigneron et al. that exclusively specific peptides and not a random library of peptides can be synthesized by the proteasome from fragments present in the proteasomal cavity after degradation of proteins.[198] Thus, for proteasomal aminolysis, the reacting peptide also has to be tightly bound to the primed sites at the active center, showing that the proteasome possesses additional peptide splicing activity and is involved in the generation of noncontiguous antigenic peptides by cleaving the precursor peptide and catalyzing the formation of a peptide bond between two distant fragments. Since this process also takes place *in vitro* in the absence of exogenous ATP, the required energy must be recovered from one of the bonds cleaved by the proteasome.[198] Substrate cleavage by the proteasome is known to occur by nucleophilic attack on the peptide bond at the active site threonine, resulting in the formation of an acyl enzyme intermediate, in which a peptide fragment is attached by an ester bond to the catalytic threonine. This acyl enzyme intermediate is usually rapidly hydrolyzed. However, inside the catalytic chamber of the proteasome, the intermediate is surrounded by peptide fragments whose N termini sometimes compete with water molecules for a nucleophilic attack of the ester bond of the intermediate, which occasionally results in the formation of a new peptide bond and production of the spliced peptide.

4.10. Limitations of Applying Crystallographic Knowledge for Proteasomal Inhibitor Design

Most structural reports on selective ligand−protein interactions focus particularly on adaptation and movement of the ligand upon binding. However, the flexibility of protein residues and their concerted movements caused by ligand binding are just as crucial for stabilization of the ligand-bound state and have significant effects on IC_{50} values. Structural rearrangement of side chain residues, in particular those forming the S1 and S3 specificity pockets, was observed for proteasomal subunits $\beta2$ and $\beta5$ after binding of the inhibitor to their active centers.[81] The complexity and biological significance of molecular flexibility are illustrated by the examples of endocyclic biphenyl-ether-bridged tripeptides: binding of BIA-1a and BIA-2a to subunit $\beta2$ generates significant structural rearrangement of residues, which are not involved in the formation of the S3 pocket.[197] The rearrangement of backbone residues does not happen upon binding of TMC-95. These observations are surprising, since structural superposition of TMC-95A and BIA-1a in their bound forms shows high similarity of their constrained geometries, conformations, and binding modes. The main difference between these inhibitors is that the endocyclic biphenyl ether compounds lack the functional oxindole group present in the TMC-95A structure (Figure 8c2). The absence of this functional group seems to lead to the destabilization of the extended β-type backbone conformation. In the endocyclic biphenyl ether−proteasome complex, the ligand is stabilized by formation of four hydrogen bonds with the Glu22 residue of subunit $\beta2$ (Figure 8d2). Interestingly, the BIA-1a and BIA-2a compounds differ in the structural orientation of the endocyclic biphenyl ether clamp, which is not involved in formation of hydrogen bonds but is essential for high affinity binding.

In the case of β-lactones, the binding modes of the inhibitors omuralide and homobelactosin C are the same, but the inhibition mechanism of the inhibitors differs significantly. Both inhibitors displace the nucleophilic water molecule, thus preventing hydrolysis of the ester bond, but in a completely different manner (see also section 4.6.3). Thus, it should be kept in mind that crystallographic data can only display an average snapshot image of a protein or a protein−ligand complex, and they do not provide enough information for prediction of IC_{50} values and interaction kinetics. In most cases, data derived from crystallographic analysis are in accordance with experimentally determined IC_{50} values. However, proteasomal proteolytic activity assays are generally performed with small fluorogenic peptides, which do not represent the natural proteasomal substrates and are poorly degraded by proteasomes.

In addition, the effectiveness of *in vitro* activity assays significantly depends on buffer conditions and substrate mimetics. All that explains often observed significant differences in kinetic measurements of enzyme activity and structural predictions of the ligand binding efficiency or affinity. In proteasomes, the rate-limiting step in proteolysis is defined by substrate accessibility to the proteolytically active centers, whereas binding of substrates to the specificity pockets only plays a minor role in protein turnover rates.[77,78] Once the selected and unfolded proteins have entered the central proteolytic chamber of the proteasome, their affinity for the distinct specificity pockets (defined by the primary sequence) determines the resulting product cleavage pattern. Thus, it is the amino acid sequence which determines at which active sites the peptide bond hydrolysis will be performed,[79] so that the cleavage pattern for each protein is unique. So far, it is still not possible to predict the proteasomal cleavage patterns of proteins just from their primary sequence. This is a major challenge for the future, since this knowledge would have a great impact on immunology and cell communication research, allowing prediction of epitopes or signal transduction peptides from primary sequences.

5. Biological Role and Medical Implementations of Proteasomal Inhibitors

The availability of proteasomal inhibitors with increasing specificity and potency has generated a large collection of data documenting the critical role of the proteasomal−ubiquitin protein degradation pathway in many biological processes. When applied to cells, proteasomal inhibitors elicit diverse biological effects, depending on the process which is the most affected. The ultimate effect of proteasomal inhibitors depends on several parameters, such as cell type and the proliferation status, nature, and dose of the inhibitor and the time of the exposure.[199] The estimation of the overall biological effect of the inhibitor treatment should be made cautiously, since many of the inhibitors affect not only the proteasome but also other cytosolic proteases. As has been discussed in previous sections, peptide aldehydes and vinyl sulfones, for example, are also able to inhibit the activity of proteases such as cathepsins and calpains. Lactacystin, which was originally thought to be specific only for the proteasome, was shown later to also inhibit cathepsin A.[200] Here we will briefly describe the effect of proteasomal inhibitors on various essential cellular processes, highlighting their existing and theoretical biomedical implications.

5.1. Cell Cycle Control

The proteasome is involved in degradation of numerous proteins regulating the cell cycle (G1 and mitotic cyclins, CDK inhibitors, p53, etc.). Inhibition of the proteasomal activity was reported to stop the cell cycle at different stages: there are reports of arrested mitosis at the G1/S boundary and G2/transition.[165,201,202] Treatment of oocytes with proteasomal inhibitors such as lactacystin and MG132 disrupted the process of oocyte meiosis and early cleavage in many aspects, including normal organization of the spindle at the prophase and segregation of chromosomes at the anaphase for normal meiosis.[203−205] Interestingly, proteasomal inhibitors were also found to completely block fertilization of the oocyte: sperm penetration into the oocytes was impossible when inhibitors were added at the beginning of insemination.[206]

5.2. Apoptosis

Apoptotic cell death has always been attributed to the activation of a cascade of cytoplasmic proteases, which cleave a number of target proteins. Usage of proteasomal inhibitors, though, has demonstrated that the proteasomal−ubiquitin pathway has a decisive effect on cell death and survival. The identification and development of proteasome specific inhibitors has provided new tools for more direct investigations of apoptotic cell death. Effects of proteasomal inhibitors on apoptosis strongly depend on the proliferation status of the cell and the cell types (reviewed in ref 207). Various substrates in the ubiquitin-dependent proteasomal degradation pathway (p53, E2F, c-myc, c-jun, NF-κB) are short-lived proteins which are critical for cell progression and transcriptional regulation, and under certain conditions, they also become the key players in the control of the cell death program. Consequently, modulation of the intracellular level of these proteins will have drastic effects on cell survival. Proteasomal inhibitors often trigger apoptosis in proliferating cells, probably since they can stabilize both positive and negative regulators of cell growth and thereby stimulate conflicting signaling pathways.[208] However, in some cases, for example in terminally differentiated or nonproliferating cells, proteasomal inhibitors protect cells against apoptosis.[209,210] The pro- and anti-apoptotic effects of the proteasomal inhibitors seem to be cell specific, probably because the stabilization of many proteins which are critical for cellular growth, homeostasis, and defense, including p53 and NF-κB, has a differential effect impact according to the cellular context. In general, rapidly dividing cells are more sensitive to pro-apoptotic effects of proteasome inhibitors than nondividing ones.[211,212] For example, SV-40 transformed fibroblasts, but not normal fibroblasts, are susceptible to inhibitor-induced apoptosis,[213] and 340-fold higher concentrations of inhibitors are necessary to induce apoptosis in quiescent primary endothelial cells, as compared to proliferating cells.[214] It was also shown that accumulation of unfolded nondegraded proteins upon treatment of cells with proteasomal inhibitors leads to activation of the stress kinase c-Jun N-terminal kinase (JNK), which can turn on the apoptotic cascade.[215]

Selective and cell specific activation of apoptosis by proteasome inhibitors allowed their use as tumor suppressors. Some inhibitors were shown to efficiently induce apoptosis in many tumor cells, whereas untransformed cells remained unharmed.

5.3. Induction of Heat Shock Response

At non-apoptotic concentrations, proteasome inhibitors were shown to protect cells against apoptosis induced by other factors.[199] An interesting link between the anti-apoptotic properties of proteasome inhibitors and accumulation of heat-shock proteins (hsp) has been suggested, since inhibitor treatment induced the production of proteins of the hsp family.[216] In this study, exposure of Madin−Darby canine kidney cells to various proteasome inhibitors, including the peptide aldehydes (MG132, MG115, *N*-acetyl-Leu−Leu-nLeu-al) and lactacystin, inhibited the degradation of short-lived proteins and increased markedly the levels of mRNAs encoding cytosolic heat-shock proteins (Hsp70, polyubiquitin) and ER chaperones (BiP, Grp94, ERp72). Moreover, induction of heat shock proteins stimulated cells' thermotolerance: treatment of cells with MG132 for as little as 2 hours markedly increased the survival of cells subjected to high temperatures (up to 46 °C). Thus, proteasomal inhibitors may have applications in protection against cell injury, various stress situations, and apoptosis.[215,217]

5.4. Transcription Activation

Ongoing research brings every day new evidence that the role of the proteasome is not limited to protein degradation and that this multifunctional proteolytic complex is involved in many different essential cellular processes. According to recently published data, the proteasome is actively involved in the gene expression control by the nuclear hormone receptor (NR)-mediated transcriptional regulation (reviewed in ref 218). The proteasome may also function in transcription elongation, since it was shown that it interacts with both RNA polymerase II and the transcription elongation factor Cdc68.[219,220] This role, though, is attributed to the 19S regulator, and it was shown that mutations in the 19S regulatory particle cause defects in elongation.[221] In addition to its role in transcription, the proteasome was shown to interact with the ubiquitin-like domain of the nucleotide excision repair (NER) protein Rad23. These interactions are required for optimal functioning of the protein and are independent of the proteolytic activities of the proteasome.[222] Moreover, the recent study has shown that the proteasome is involved in recruitment of the promoter activating complex SAGA in yeast.[223]

5.5. Inhibition of Antigen Presentation

Proteasomes play a major role in the cellular immune response, since they represent the main producer of antigenic peptides.[224] Protein degradation is the source of the 8−10 amino acids long antigenic peptides presented on the surface of the cell by MHC class I receptors. The first *in vivo* study of proteasomal inhibitors demonstrated that blocking the proteasome reduces the generation of peptides used in MHC class I antigen presentation.[106] The proteasome hence qualifies as a target for modifying or silencing antigen processing and presentation to cytotoxic T cells, which are important players in transplant rejection and autoimmune diseases. Thus, novel and selective proteasome inhibitors could have strong potential as drugs for suppressing or modifying the cytotoxic immune response.[225]

5.6. Anticancer Therapy

Disregulation of the ubiquitin−proteasomal protein degradation pathway causes onset of numerous inherited and

acquired diseases such as Alzheimer's disease, amyotropic lateral sclerosis, asthma, several types of cancer, autoimmune thyroid disease, type I diabetes, ischemia-reperfusion injury, cachexia, graft rejection, hepatitis B, inflammatory bowel disease, and sepsis (reviewed in refs 132 and 226−228). Application of different proteasomal inhibitors alone and in combination with other drugs has proved to be helpful in treatment of different diseases. The effects of the inhibitors are often associated with suppression of angiogenesis. In normal differentiated adult cells, the control of angiogenic pathways is tightly regulated and, generally, blood vessel growth is not stimulated unless injury occurs. However, cancerous tissues stimulate angiogenesis that in turn leads to increased tumor formation and possible metastases. Many of the factors involved in angiogenesis are regulated by the proteasome. Thus, inhibition of the proteasome activity has been found to inhibit angiogenesis and induce apoptosis in human cancer cells with limited toxicity to normal cells. Therefore, the dual action of blocking angiogenesis and inducing cell death makes proteasome inhibition an attractive modality for chemotherapy. A variety of proteasome inhibitors have been studied such as lactacystin, salinosporamide A, and the boronic acid bortezomib (MLN-341), which have already been approved in the United States as prescriptive drugs for use against relapsed and/or refractory multiple myeloma (MM).[229] There exists much experimental evidence that bortezomib is also effective in treatment of other types of cancer—hematologic malignancies, such as non-Hodgkin's lymphomas, different types of sold tumors,[230] and osteolytic skeletal metastases—especially when treatment is initiated early during the disease process.[231] Bortezomib was shown to reverse development of Mantle Cell Lymphoma (MCL), which is a mature B-cell lymphoma with an aggressive course and generally poor prognosis. Conventional chemotherapy has little efficacy against this type of cancer.[232] Usage of bortezomib has proved to be effective in various lung cancer cell lines, especially in combination with other antitumor agents such as taxanes, gemcitabine, carboplatin, histone deactylase inhibitors, and other molecularly targeted agents (reviewed in ref 233). Several recent studies demonstrate that a combination of two proteasomal inhibitors or a combination of an inhibitor and other antitumor agents gives the best therapeutic results, providing the synergistic effect of both agents. For example, tubacin (inhibitor of aggresomes) combined with bortezomib mediates significant anti-MM activity, providing the framework for clinical evaluation of combined therapy to improve patient outcome in multiple myeloma.[234]

Though bortezomib therapy has proven to be successful for the treatment of multiple myeloma and potentially good for other types of cancer, prolonged treatment is associated with toxicity and development of drug resistance. A novel proteasome inhibitor NPI-0052 (salinosporamide A) induces apoptosis in MM cells resistant to conventional and bortezomib therapies.[172,174] NPI-0052 is distinct from bortezomib in its chemical structure, effects on proteasome activities, mechanisms of action, and toxicity profile against normal cells. Moreover, NPI-0052 is orally bioactive. In animal tumor model studies, NPI-0052 is well tolerated and prolongs survival, with significantly reduced tumor recurrence. Combining NPI-0052 and bortezomib induces synergistic anti-MM activity.[174]

Other widely used proteasomal inhibitors with potential to become anticancer drugs are MG-132 and lactacystin. Combinations of the proteasomal inhibitor MG132 and the apoptotic stimuli such as rhTRAIL (recombinant human TNF-related apoptosis inducing ligand) were shown to be potentially therapeutically useful in cervical cancer treatment.[235] MG132 has potential for prevention of vascular restenosis[236] and human pancreatic cancer.[237] Recently, it was reported that prostate cancer cells demonstrate a significant increase in apoptosis when treated with increasing levels of lactacystin, MG132, or a combination of sublethal doses of these two inhibitors.[238]

The development of new proteasomal inhibitors with perspectives for cancer treatment is one of the fastest growing fields in modern biomedical science. Most recently, certain classes of copper compounds have been found to act as potent proteasome inhibitors. The potential of particular organic compounds, such as 8-hydroxyquinoline, to spontaneously bind with tumor cellular copper and form proteasome inhibitors provides a new modality of anti-proteasome and anti-angiogenesis chemotherapy (reviewed in ref 239).

5.7. Antiviral Effects of Proteasomal Inhibitors

Successful usage of proteasomal inhibitors in cancer therapy stimulated clinical research toward treatment of other diseases including widespread diseases caused by various viruses. The family of Paramyxoviridae contains viruses that induce a wide range of distinct clinical illnesses in humans such as measles virus, which in rare instances is followed by subacute sclerosing panencephalitis (SSPE), mumps virus, which has symptoms of parotitis, orchitis, and encephalitis, and the parainfluenza viruses which are respiratory pathogens. Paramyxovirus infections can be detected worldwide, and currently there are no specific therapeutic treatments or vaccines available for many of these diseases. In a recent study, treatment of different virus-infected cells with different concentrations of MG132 and lactacystin reduced viral growth in a dose-dependent manner.[240] Release of vesicular stomatitis virus showed high susceptibility to MG132 and release of influenza virus A/WSN/33 was only mildly susceptible to the drug in LLC-MK2 cells. Effects of proteasome inhibitors on virus maturation were shown to be highly cell specific and partly virus specific, and they provide the basis for further investigations of proteasome inhibitors as potential antiviral drugs.

A dipeptidyl boronic acid proteasome inhibitor, named MLN-273, was tested on blood and liver stages of Plasmodium parasite species which cause malaria.[241] The inhibitor blocked development of the parasites at different stages but did not injure uninfected erythrocytes and hepatocytes. These data may provide a good basis for development of boronic acid derivatives as drugs, for example, for malaria chemotherapy.

Furthermore, it was demonstrated that maturation and budding of human immunodeficiency virus types 1 (HIV-1) and 2, simian immunodeficiency virus, and Rous sarcoma virus, as well as murine leukemia virus and Mason−Pfizer monkey virus, are reduced by proteasomal inhibitors.[242,243] Proteasome inhibitors can affect the budding of a virus that assembles within the cytoplasm. However, the budding of a mouse mammary tumor virus was unaffected by proteasome inhibitors, similar to the proteasome-independent budding previously observed for equine infectious anaemia virus. For all the cell lines tested, the inhibitor treatment effectively inactivated proteasomes, as measured by the accumulation of poly-ubiquitinated proteins.[243] The ubiquitination system

was also inhibited, as evidenced by the loss of mono-ubiquitinated histones from treated cells. The effect of the inhibitors appears to be indirect, due to the depletion of the pool of free ubiquitin, whose conjugation to viral Gag proteins is required for virus release from the cell but does not target Gag proteins for proteasomal degradation. Thus, proteasomal inhibitors might represent a possible drug candidate for the treatment of HIV infection.

5.8. Ischemic Stroke

The ubiquitin−proteasomal system plays a critical role in cerebral ischemic injury. Ischemic and hypoxic trauma, and their associated oxidative, nitrosylative, and energetic stress, underlie neurodegeneration following stroke and evoke a discrete set of transcriptional events which have a complex and interdependent relationship with proteasomal function. Rapid elimination of denatured, misfolded, and damaged proteins by the proteasome becomes a critical determinant of cell fate. Proteasome inhibitors, such as MLN519, were shown to reduce neuronal and astrocytic degeneration, cortical infarct volume, and infarct neutrophil infiltration in animal models of cerebral ischemia **(**reviewed in refs 244 and 245). MLN519 is currently undergoing clinical research studies as a potential drug against stroke.[246] However, long-lasting changes in proteasomal function are not recommended, since there is evidence implicating long-term proteasomal dysfunction in chronic neurodegenerative disease. Development of short-lived proteasome inhibitors, or compounds which can spatially and temporally regulate the activity of the proteasome, would open new perspectives for treatment of acute neurological diseases, including ischemic stroke.

5.9. Anti-inflammatory Effect

Due to the prominent role of the transcription factor NF-kappaB in inflammatory response, proteasome inhibitors may be used as anti-inflammatory agents, since they strongly stabilize its inhibitor IkappaBalpha (reviewed in ref 247). In quiescent cells, NF-kappaB exists in a latent form and is activated via a signal-dependent proteolytic mechanism in which the inhibitory protein IkappaBalpha is degraded by the ubiquitin−proteasome pathway. Bortezomib was shown to inhibit the activation of NF-kappaB and the subsequent transcription of genes that are regulated by NF-kappaB.[248] Oral administration of PS-341 had anti-inflammatory effects in a model of streptococcal cell wall-induced polyarthritis and liver inflammation in rats.

5.10. Multifunctional Proteasome Inhibitor Cocktails

In addition to the great variety of natural and synthetic proteasomal inhibitors described in this article, there exist small molecules (natural or synthetic compounds) binding far away from the proteasomal catalytic centers yet modifying the performance of the proteasome. Most such compounds are allosteric effectors capable of regulating the proteasome *in vitro* and *in vivo* in a manner more diverse and precise than that of competitive inhibitors. Proline- and arginine-rich peptides (PR peptides) are examples of such compounds and are currently being considered as potential drugs with anti-inflammatory and pro-angiogenic activities.[249] A combination of these small indirect inhibitors with competitive proteasome inhibitors can provide an excellent basis for development of new proteasomal inhibitor cocktails and possible therapeutic applications.

5.11. Tuberculosis and Proteasome Inhibitors

About two billion people are infected with *Mycobacterium tuberculosis*. The identification of pathways used by this microorganism to resist elimination by the host immune response has been the main challenge for researchers. The latest studies showed that at least six different pathways are individually essential and nonredundant for resistance of Mtb to acidified nitrite, which is produced by macrophages and represents a physiologic antimicrobial system.[250] Among these pathways is the proteasome, which apparently protects the bacteria from oxidative stress. It was shown that inhibition of the *Mycobacterium tuberculosis* markedly sensitized the pathogen to the antibacterial chemistries of the host. The following efforts identified dipeptidyl boronate *N*-(4-morpholine)carbonyl-β-(1-naphthyl)-L-alanine-L-leucine boronic acid (MLN-273), an analogue of the antimyeloma drug Bortezomib, as an effective inhibitor of *Mycobacterium* proteasome,[138] which opens perspectives for chemotherapy for this life threatening disease with proteasomal inhibitor-based drugs.

6. Conclusions and Perspectives

The proteasome plays an essential role in the turnover of cellular proteins. Modulation and inhibition of proteasomal activity are thus promising ways to retard or block degradation of specific proteins to correct diverse pathologies. The prominent role of the proteasome in proliferation and in inflammation suggests the potential to exploit proteasomal inhibitors as anti-tumor, pro-apoptotic, or anti-inflammatory agents. As mentioned above, encouraging anti-inflammatory and anti-tumor effects have already been obtained with some proteasomal inhibitors. Modern methods of elucidation of the three-dimensional structure of proteasomal inhibitors in their free state and in complex with the proteasome provide valuable information on the flexibility of residues of the compound and the protein upon complex formation. This structural information is extensively used for improvement of existing inhibitors and design of new compounds.

Though nowadays there exist quite a number of selective and efficient proteasomal inhibitors, the toxic side effects of these compounds strongly limit their potential in possible disease treatment. One possibility to influence proteasomal substrate specificity might be the modulation of activity of the 19S regulatory particle and associated proteins. Furthermore, structural data provide insights for creation of inhibitors which target only specific proteasomal active sites, thus opening opportunities to alter the pattern of generated peptide products, which in turn might affect downstream signal transduction processes. Other fields which still need to be explored are endogenous inhibitors of the proteasome. So far there are few data available in this respect, and it is possible that new molecules will be discovered which might specifically modulate proteasome-dependent turnover of specific proteins.

7. Acknowledgments

We thank Barbara Potts (Nereus Pharmaceuticals, San Diego, CA) for critical reading of our manuscript and for sharing with us her extensive chemical knowledge in the field of proteasome inhibition.

8. References

(1) Etlinger, J.; Goldberg, A. *Proc. Natl. Acad. Sci. U.S.A.* **1977**, *74*, 54.
(2) Hershko, A.; Leshinsky, E.; Ganoth, D.; Heller, H. *Proc. Natl. Acad. Sci. U.S.A.* **1984**, *81*, 1619.
(3) Hough, R.; Rechsteiner, M. *Proc. Natl. Acad. Sci. U.S.A.* **1984**, *81*, 90.
(4) Hershko, A.; Ciechanover, A. *Annu. Rev. Biochem.* **1998**, *67*, 425.
(5) Haas, A. L.; Warms, J. V.; Hershko, A.; Rose, I. A. *J. Biol. Chem.* **1982**, *257*, 2543.
(6) Huang, Y.; Baker, R. T.; Fischer-Vize, J. A. *Science* **1995**, *270*, 1828.
(7) Keiler, K.; Waller, P.; Sauer, R. *Science* **1996**, *271*, 990.
(8) Karzai, A.; Roche, E.; Sauer, R. *Nat. Struct. Biol.* **2000**, *7*, 449.
(9) Coux, O.; Tanaka, K.; Goldberg, A. L. *Annu. Rev. Biochem.* **1996**, *65*, 801.
(10) Voges, D.; Zwickl, P.; Baumeister, W. *Annu. Rev. Biochem.* **1999**, *68*, 1015.
(11) Deveraux, Q.; Ustrell, V.; Pickart, C.; Rechsteiner, M. *J. Biol. Chem.* **1994**, *272*, 182.
(12) Lam, Y. A.; DeMartino, G. N.; Pickart, C. M.; Cohen, R. E. *J. Biol. Chem.* **1997**, *272*, 28438.
(13) Rubin, D. M.; Glickman, M. H.; Larsen, C. N.; Dhruvakumar, S.; Finley, D. *EMBO J.* **1998**, *17*, 4909.
(14) DeMartino, G. N.; Slaughter, C. A. *J. Biol. Chem.* **1999**, *274*, 22123.
(15) Ustrell, V.; Hoffman, L.; Pratt, G.; Rechsteiner, M. *EMBO J.* **2002**, *21*, 3516.
(16) Hendil, K. B.; Khan, S.; Tanaka, K. *Biochem. J.* **1998**, *332*, 749.
(17) Charette, M.; Henderson, G.; Markovitz, A. *Proc. Natl. Acad. Sci. U.S.A.* **1981**, *78*, 4728.
(18) Waxman, L.; Goldberg, A. L. *Proc. Natl. Acad. Sci. U.S.A.* **1982**, *79*, 4883.
(19) Tomoyasu, T.; Gamer, J.; Bukau, B.; Kanemori, M.; Mori, H.; Rutman, A.; Oppenheim, A.; Yura, T.; Yamanaka, K.; Niki, H.; et al. *EMBO J.* **1995**, *14*, 2551.
(20) Bieniossek, C.; Schalch, T.; Bumann, M.; Meister, M.; Meier, R.; Baumann, U. *Proc. Natl. Acad. Sci. U.S.A.* **2006**, *103*, 3066.
(21) Rohrwild, M.; Coux, O.; Huang, H. C.; Moerschell, R. P.; Yoo, S. J.; Seol, J. H.; Chung, C. H.; Goldberg, A. L. *Proc. Natl. Acad. Sci. U.S.A.* **1996**, *93*, 5808.
(22) Bochtler, M.; Hartmann, C.; Song, H. K.; Bourenkov, G. P.; Bartunik, H. D.; Huber, R. *Nature* **2000**, *403*, 800.
(23) Sousa, M. C.; Trame, C. B.; Tsuruta, H.; Wilbanks, S. M.; Reddy, V. S.; McKay, D. B. *Cell* **2000**, *103*, 633.
(24) Wu, W. F.; Zhou, Y.; Gottesman, S. *J. Bacteriol.* **1999**, *181*, 3687.
(25) Glas, R.; Bogyo, M.; McMaster, J. S.; Gaczynska, M.; Ploegh, H. L. *Nature* **1998**, *392*, 618.
(26) Tamura, T.; Tamura, N.; Cejka, Z.; Hegerl, R.; Lottspeich, F.; Baumeister, W. *Science* **1996**, *274*, 1385.
(27) Brandstetter, H.; Kim, J. S.; Groll, M.; Huber, R. *Nature* **2001**, *414*, 466.
(28) Kim, J. S.; Groll, M.; Musiol, H. J.; Behrendt, R.; Kaiser, M.; Moroder, L.; Huber, R.; Brandstetter, H. *J. Mol. Biol.* **2002**, *324*, 1041.
(29) Göttig, P.; Groll, M.; Kim, J. S.; Huber, R.; Brandstetter, H. *EMBO J.* **2002**, *21*, 5343.
(30) Göttig, P.; Brandstetter, H.; Groll, M.; Gohring, W.; Konarev, P. V.; Svergun, D. I.; Huber, R.; Kim, J. S. *J. Biol. Chem.* **2005**, *280*, 33387.
(31) Tamura, N.; Lottspeich, F.; Baumeister, W.; Tamura, T. *Cell* **1998**, *95*, 637.
(32) Geier, E.; Pfeifer, G.; Wilm, M.; Lucchiari-Hartz, M.; Baumeister, W.; Eichmann, K.; Niedermann, G. *Science* **1999**, *283*, 978.
(33) Rockel, B.; Peters, J.; Muller, S. A.; Seyit, G.; Ringler, P.; Hegerl, R.; Glaeser, R. M.; Baumeister, W. *Proc. Natl. Acad. Sci. U.S.A.* **2005**, *102*, 10135.
(34) Kloetzel, P. M. *Nat. Immunol.* **2004**, *5*, 661.
(35) Franzetti, B.; Schoehn, G.; Hernandez, J.; Jaquinod, M.; Ruigrok, R.; Zaccai, G. *EMBO J.* **2002**, *21*, 2132.
(36) Borissenko, L.; Groll, M. *J. Mol. Biol.* **2005**, *346*, 1207.
(37) Russo, S.; Baumann, U. *J. Biol. Chem.* **2004**, *279*, 51275.
(38) Schwartz, A. L.; Ciechanover, A. *Annu. Rev. Med.* **1999**, *50*, 57.
(39) Lee, D. H.; Goldberg, A. L. *Trends Cell Biol.* **1998**, *8*, 397.
(40) Hough, R.; Pratt, G.; Rechsteiner, M. *J. Biol. Chem.* **1986**, *261*, 2408.
(41) Hough, R.; Pratt, G.; Rechsteiner, M. *J. Biol. Chem.* **1987**, *262*, 8303.
(42) Eytan, E.; Ganoth, D.; Armon, T.; Hershko, A. *Proc. Natl. Acad. Sci. U.S.A.* **1989**, *86*, 7751.
(43) Harris, J. *Biochim. Biophys. Acta.* **1968**, *150*, 534.
(44) Hegerl, R.; Pfeifer, G.; Puhler, G.; Dahlmann, B.; Baumeister, W. *FEBS Lett.* **1991**, *283*, 117.
(45) Löwe, J.; Stock, D.; Jap, B.; Zwickl, P.; Baumeister, W.; Huber, R. *Science* **1995**, *268*, 533.
(46) Groll, M.; Brandstetter, H.; Bartunik, H.; Bourenkow, G.; Huber, R. *J. Mol. Biol.* **2003**, *327*, 75.
(47) Kwon, Y.; Nagy, I.; Adams, P.; Baumeister, W.; Jap, B. *J. Mol. Biol.* **2004**, *335*, 233.
(48) Kwon, A.; Kessler, B.; Overkleeft, H.; McKay, D. *J. Mol. Biol.* **2003**, *330*, 185.
(49) Bochtler, M.; Ditzel, L.; Groll, M.; Huber, R. *Proc. Natl. Acad. Sci. U.S.A.* **1997**, *94*, 6070.
(50) Groll, M.; Ditzel, L.; Löwe, J.; Stock, D.; Bochtler, M.; Bartunik, H. D.; Huber, R. *Nature* **1997**, *386*, 463.
(51) Unno, M.; Mizushima, T.; Morimoto, Y.; Tomisugi, Y.; Tanaka, K.; Yasuoka, N.; Tsukihara, T. *Structure* **2002**, *10* (5), 609.
(52) Groll, M.; Huber, R. *Methods Enzymol.* **2005**, *398*, 329.
(53) Brown, M. G.; Driscoll, J.; Monaco, J. J. *Nature* **1991**, *353*, 355.
(54) Ortiz-Navarrete, V.; Seelig, A.; Gernold, M.; Frentzel, S.; Kloetzel, P. M.; Hammerling, G. J. *Nature* **1991**, *353*, 662.
(55) Frentzel, S.; Graf, U.; Hammerling, G. J.; Kloetzel, P. M. *FEBS Lett.* **1992**, *302*, 121.
(56) Yang, Y.; Waters, J. B.; Fruh, K.; Peterson, P. A. *Proc. Natl. Acad. Sci. U.S.A.* **1992**, *89*, 4928.
(57) Gaczynska, M.; Rock, K. L.; Goldberg, A. L. *Nature* **1993**, *365*, 264.
(58) Schmidtke, G.; Kraft, R.; Kostka, S.; Henklein, P.; Frommel, C.; Löwe, J.; Huber, R.; Kloetzel, P. M.; Schmidt, M. *EMBO J.* **1996**, *15*, 6887.
(59) Schmidtke, G.; Schmidt, M.; Kloetzel, P. M. *J. Mol. Biol.* **1997**, *268*, 95.
(60) Aki, M.; Shimbara, N.; Takashina, M.; Akiyama, K.; Kagawa, S.; Tamura, T.; Tanahashi, N.; Yoshimura, T.; Tanaka, K.; Ichihara, A. *J. Biochem. (Tokyo)* **1994**, *115*, 257.
(61) Akiyama, K.; Kagawa, S.; Tamura, T.; Shimbara, N.; Takashina, M.; Kristensen, P.; Hendil, K. B.; Tanaka, K.; Ichihara, A. *FEBS Lett.* **1994**, *343*, 85.
(62) Brannigan, J. A.; Dodson, G.; Duggleby, H. J.; Moody, P. C.; Smith, J. L.; Tomchick, D. R.; Murzin, A. G. *Nature* **1995**, *378*, 416.
(63) Groll, M.; Heinemeyer, W.; Jager, S.; Ullrich, T.; Bochtler, M.; Wolf, D. H.; Huber, R. *Proc. Natl. Acad. Sci. U.S.A.* **1999**, *96*, 10976.
(64) Ditzel, L.; Stock, D.; Löwe, J. *Biol. Chem.* **1997**, *378*, 239.
(65) Chen, P.; Hochstrasser, M. *Cell* **1996**, *86*, 961.
(66) Jäger, S.; Groll, M.; Huber, R.; Wolf, D. H.; Heinemeyer, W. *J. Mol. Biol.* **1999**, *291*, 997.
(67) Arendt, C. S.; Hochstrasser, M. *EMBO J.* **1999**, *18*, 3575.
(68) Seemüller, E.; Lupas, A.; Stock, D.; Löwe, J.; Huber, R.; Baumeister, W. *Science* **1995**, *268*, 579.
(69) Ditzel, L.; Huber, R.; Mann, K.; Heinemeyer, W.; Wolf, D. H.; Groll, M. *J. Mol. Biol.* **1998**, *279*, 1187.
(70) Groll, M.; Huber, R.; Potts, B. C. *J. Am. Chem. Soc.* **2006**, *128*, 5136.
(71) Duggleby, H. J.; Tolley, S. P.; Hill, C.; Dodson, E. J.; Dodson, G.; Moody, P. C. *Nature* **1995**, *373*, 264.
(72) Chen, P.; Hochstrasser, M. *EMBO J.* **1995**, *14*, 2620.
(73) Seemüller, E.; Lupas, A.; Baumeister, W. *Nature* **1996**, *382*, 468.
(74) Huber, R.; Bode, W. *Acc. Chem. Res.* **1978**, *11*, 114.
(75) Heinemeyer, W.; Fischer, M.; Krimmer, T.; Stachon, U.; Wolf, D. H. *J. Biol. Chem.* **1997**, *272*, 25200.
(76) Nussbaum, A. K.; Dick, T. P.; Keilholz, W.; Schirle, M.; Stevanovic, S.; Dietz, K.; Heinemeyer, W.; Groll, M.; Wolf, D. H.; Huber, R.; Rammensee, H. G.; Schild, H. *Proc. Natl. Acad. Sci. U.S.A.* **1998**, *95*, 12504.
(77) Groll, M.; Bajorek, M.; Kohler, A.; Moroder, L.; Rubin, D. M.; Huber, R.; Glickman, M. H.; Finley, D. *Nat. Struct. Biol.* **2000**, *7*, 1062.
(78) Whitby, F. G.; Masters, E. I.; Kramer, L.; Knowlton, J. R.; Yao, Y.; Wang, C. C.; Hill, C. P. *Nature* **2000**, *408*, 115.
(79) Kisselev, A. F.; Callard, A.; Goldberg, A. L. *J. Biol. Chem.* **2006**, *281*, 8582.
(80) Jager, S.; Groll, M.; Huber, R.; Wolf, D. H.; Heinemeyer, W. *J. Mol. Biol.* **1999**, *291*, 997.
(81) Groll, M.; Huber, R. *Biochim. Biophys. Acta* **2004**, *1695*, 33.
(82) Orlowski, M.; Cardozo, C.; Michaud, C. *Biochemistry* **1993**, *32*, 1563.
(83) Arendt, C. S.; Hochstrasser, M. *Proc. Natl. Acad. Sci. U.S.A.* **1997**, *94*, 7156.
(84) Hilt, W.; Wolf, D. H. *Trends Biochem. Sci.* **1996**, *21*, 96.
(85) Dick, T. P.; Nussbaum, A. K.; Deeg, M.; Heinemeyer, W.; Groll, M.; Schirle, M.; Keilholz, W.; Stevanovic, S.; Wolf, D. H.; Huber, R.; Rammensee, H. G.; Schild, H. *J. Biol. Chem.* **1998**, *273*, 25637.
(86) Michalek, M. T.; Grant, E. P.; Gramm, C.; Goldberg, A. L.; Rock, K. L. *Nature* **1993**, *363*, 552.
(87) Fehling, H. J.; Swat, W.; Laplace, C.; Kuhn, R.; Rajewsky, K.; Muller, U.; von Boehmer, H. *Science* **1994**, *265*, 1234.
(88) Sibille, C.; Gould, K. G.; Willard-Gallo, K.; Thomson, S.; Rivett, A. J.; Powis, S.; Butcher, G. W.; De Baetselier, P. *Curr. Biol.* **1995**, *5*, 923.

(89) Nandi, D.; Jiang, H.; Monaco, J. J. *J. Immunol.* **1996**, *156*, 2361.
(90) Groettrup, M.; Kraft, R.; Kostka, S.; Standera, S.; Stohwasser, R.; Kloetzel, P. M. *Eur. J. Immunol.* **1996**, *26*, 863.
(91) Boes, B.; Hengel, H.; Ruppert, T.; Multhaup, G.; Koszinowski, U. H.; Kloetzel, P. M. *J. Exp. Med.* **1994**, *179*, 901.
(92) York, I. A.; Rock, K. L. *Annu. Rev. Immunol.* **1996**, *14*, 369.
(93) Beninga, J.; Rock, K. L.; Goldberg, A. L. *J. Biol. Chem.* **1998**, *273*, 18734.
(94) Groll, M.; Larionov, O. V.; Huber, R.; de Meijere, A. *Proc. Natl. Acad. Sci. U.S.A.* **2006**, *103*, 4576.
(95) Silver, M. L.; Parker, K. C.; Wiley, D. C. *Nature* **1991**, *350*, 619.
(96) Engelhard, V. H. *Curr. Opin. Immunol.* **1994**, *6*, 13.
(97) Driscoll, J.; Brown, M. G.; Finley, D.; Monaco, J. J. *Nature* **1993**, *365*, 262.
(98) Van Kaer, L.; Ashton-Rickardt, P.; Eichelberger, M.; Gaczynska, M.; Nagashima, K.; Rock, K.; Goldberg, A.; Doherty, P.; Tonegawa, S. *Immunity* **1994**, *1*, 533.
(99) Sykulev, Y.; Joo, M.; Vturina, I.; Tsomides, T. J.; Eisen, H. N. *Immunity* **1996**, *4*, 565.
(100) Vinitsky, A.; Michaud, C.; Powers, J. C.; Orlowski, M. *Biochemistry* **1992**, *31*, 9421.
(101) Palmer, J. T.; Rasnick, D.; Klaus, J. L.; Bromme, D. *J. Med. Chem.* **1995**, *38*, 3193.
(102) Adams, J.; Behnke, M.; Chen, S.; Cruickshank, A. A.; Dick, L. R.; Grenier, L.; Klunder, J. M.; Ma, Y. T.; Plamondon, L.; Stein, R. L. *Bioorg. Med. Chem. Lett.* **1998**, *8*, 333−8.
(103) Cardozo, C.; Vinitsky, A.; Hidalgo, M. C.; Michaud, C.; Orlowski, M. *Biochemistry* **1992**, *31*, 7373.
(104) Donkor, I. O. *Curr. Med. Chem.* **2000**, *7*, 1171.
(105) Shaw, E. *Adv. Enzymol. Relat. Areas Mol. Biol.* **1990**, *63*, 271.
(106) Rock, K. L.; Gramm, C.; Rothstein, L.; Clark, K.; Stein, R.; Dick, L.; Hwang, D.; Goldberg, A. L. *Cell* **1994**, *78*, 761.
(107) Lee, D. H.; Goldberg, A. L. *J. Biol. Chem.* **1996**, *271*, 27280.
(108) Harding, C. V.; France, J.; Song, R.; Farah, J. M.; Chatterjee, S.; Iqbal, M.; Siman, R. *J. Immunol.* **1995**, *155*, 1767.
(109) Palombella, V. J.; Rando, O. J.; Goldberg, A. L.; Maniatis, T. *Cell* **1994**, *78*, 773.
(110) Tsubuki, S.; Saito, Y.; Tomioka, M.; Ito, H.; Kawashima, S. *J. Biochem. (Tokyo*) **1996**, *119*, 572.
(111) Figueiredo-Pereira, M. E.; Berg, K. A.; Wilk, S. *J. Neurochem.* **1994**, *63*, 1578.
(112) Nazif, T.; Bogyo, M. *Proc. Natl. Acad. Sci. U.S.A.* **2001**, *98*, 2967.
(113) Braun, H. A.; Umbreen, S.; Groll, M.; Kuckelkorn, U.; Mlynarczuk, I.; Wigand, M. E.; Drung, I.; Kloetzel, P. M.; Schmidt, B. *J. Biol. Chem.* **2005**, *280*, 28394.
(114) Groll, M.; Bochtler, M.; Brandstetter, H.; Clausen, T.; Huber, R. *ChemBioChem* **2005**, *6*, 222.
(115) Loidl, G.; Groll, M.; Musiol, H. J.; Ditzel, L.; Huber, R.; Moroder, L. *Chem. Biol.* **1999**, *6*, 197.
(116) Wunsch, E.; Moroder, L.; Nyfeler, R.; Kalbacher, H.; Gemeiner, M. *Biol. Chem. Hoppe-Seyler* **1985**, *366*, 53.
(117) Loidl, G.; Groll, M.; Musiol, H. J.; Huber, R.; Moroder, L. *Proc. Natl. Acad. Sci. U.S.A.* **1999**, *96*, 5418.
(118) Spike, C. G.; Parry, R. W. *J. Am. Chem. Soc.* **1953**, *75*, 2726.
(119) Page, M. I.; Jencks, W. P. *Proc Natl. Acad Sci. U.S.A.* **1971**, *68*, 1678.
(120) Huber, R.; Deisenhofer, J.; Colman, P. M.; Matsushima, M.; Palm, W. *Nature* **1976**, *264*, 415.
(121) Gibson, J. F.; Ingram, D. J.; Perutz, M. F. *Nature* **1956**, *178*, 906.
(122) Bogyo, M.; McMaster, J. S.; Gaczynska, M.; Tortorella, D.; Goldberg, A. L.; Ploegh, H. *Proc. Natl. Acad. Sci. U.S.A.* **1997**, *94*, 6629.
(123) Bogyo, M.; Shin, S.; McMaster, J. S.; Ploegh, H. L. *Chem. Biol.* **1998**, *5*, 307.
(124) Ovaa, H.; van Swieten, P. F.; Kessler, B. M.; Leeuwenburgh, M. A.; Fiebiger, E.; van den Nieuwendijk, A. M.; Galardy, P. J.; van der Marel, G. A.; Ploegh, H. L.; Overkleeft, H. S. *Angew. Chem., Int. Ed.* **2003**, *42*, 3626.
(125) Kessler, B. M.; Tortorella, D.; Altun, M.; Kisselev, A. F.; Fiebiger, E.; Hekking, B. G.; Ploegh, H. L.; Overkleeft, H. S. *Chem. Biol.* **2001**, *8*, 913.
(126) Saxon, E.; Bertozzi, C. R. *Science* **2000**, *287*, 2007.
(127) Kiick, K. L.; Saxon, E.; Tirrell, D. A.; Bertozzi, C. R. *Proc. Natl. Acad. Sci. U.S.A.* **2002**, *99*, 19.
(128) Wang, E. W.; Kessler, B. M.; Borodovsky, A.; Cravatt, B. F.; Bogyo, M.; Ploegh, H. L.; Glas, R. *Proc. Natl. Acad. Sci. U.S.A.* **2000**, *97*, 9990.
(129) Groll, M.; Kim, K. B.; Kairies, N.; Huber, R.; Crews, C. M. *J. Am. Chem. Soc.* **2000**, *122*, 1237.
(130) Groll, M.; Nazif, T.; Huber, R.; Bogyo, M. *Chem. Biol.* **2002**, *9*, 655.
(131) Adams, J.; Palombella, V. J.; Sausville, E. A.; Johnson, J.; Destree, A.; Lazarus, D. D.; Maas, J.; Pien, C. S.; Prakash, S.; Elliott, P. J. *Cancer Res* **1999**, *59*, 2615.
(132) Kisselev, A. F.; Goldberg, A. L. *Chem. Biol.* **2001**, *8*, 739.
(133) McCormack, T.; Baumeister, W.; Grenier, L.; Moomaw, C.; Plamondon, L.; Pramanik, B.; Slaughter, C.; Soucy, F.; Stein, R.; Zuhl, F.; Dick, L. *J. Biol. Chem.* **1997**, *272*, 26103.
(134) Berkers, C. R.; Verdoes, M.; Lichtman, E.; Fiebiger, E.; Kessler, B. M.; Anderson, K. C.; Ploegh, H. L.; Ovaa, H.; Galardy, P. J. *Nat. Methods* **2005**, *2*, 357.
(135) Kettner, C.; Mersinger, L.; Knabb, R. *J. Biol. Chem.* **1990**, *265*, 18289.
(136) Soskel, N. T.; Watanabe, S.; Hardie, R.; Shenvi, A. B.; Punt, J. A.; Kettner, C. *Am. Rev. Respir. Dis.* **1986**, *133*, 639.
(137) Snow, R.; Bachovchin, W.; Barton, R.; Campbell, S.; Coutts, S.; Freeman, D.; Guntheil, W.; Kelly, T.; Kennedy, C.; Krolikowski, D.; Leonard, S.; Pargellis, C.; Tong, L.; Adams, J. *J. Am. Chem. Soc.* **1994**, *116*, 10860.
(138) Hu, G.; Lin, G.; Wang, M.; Dick, L.; Xu, R. M.; Nathan, C.; Li, H. *Mol. Microbiol.* **2006**, *59*, 1417.
(139) Adams, J.; Stein, R. *Annu. Rep. Med. Chem.* **1996**, *31*, 279.
(140) Groll, M.; Berkers, C. R.; Ploegh, H. L.; Ovaa, H. *Structure* **2006**, *14*, 451.
(141) Walker, B.; Lynas, J. F. *Cell. Mol. Life Sci.* **2001**, *58*, 596.
(142) London, R. E.; Gabel, S. A. *Arch. Biochem. Biophys.* **2001**, *385*, 250.
(143) London, R. E.; Gabel, S. A. *Biochemistry* **2002**, *41*, 5963.
(144) Transue, T. R.; Krahn, J. M.; Gabel, S. A.; DeRose, E. F.; London, R. E. *Biochemistry* **2004**, *43*, 2829.
(145) Elofsson, M.; Splittgerber, U.; Myung, J.; Mohan, R.; Crews, C. M. *Chem. Biol.* **1999**, *6*, 811.
(146) Kisselev, A. F.; Garcia-Calvo, M.; Overkleeft, H. S.; Peterson, E.; Pennington, M. W.; Ploegh, H. L.; Thornberry, N. A.; Goldberg, A. L. *J. Biol. Chem.* **2003**, *278*, 35869.
(147) Harris, J. L.; Alper, P. B.; Li, J.; Rechsteiner, M.; Backes, B. J. *Chem. Biol.* **2001**, *8*, 1131.
(148) Lightcap, E. S.; McCormack, T. A.; Pien, C. S.; Chau, V.; Adams, J.; Elliott, P. J. *Clin. Chem.* **2000**, *46*, 673.
(149) Sugawara, K.; Hatori, M.; Nishiyama, Y.; Tomita, K.; Kamei, H.; Konishi, M.; Oki, T. *J. Antibiot. (Tokyo*) **1990**, *43*, 8.
(150) Oikawa, T.; Hasegawa, M.; Shimamura, M.; Ashino, H.; Murota, S.; Morita, I. *Biochem. Biophys. Res. Commun.* **1991**, *181*, 1070.
(151) Hanada, M.; Sugawara, K.; Kaneta, K.; Toda, S.; Nishiyama, Y.; Tomita, K.; Yamamoto, H.; Konishi, M.; Oki, T. *J. Antibiot. (Tokyo)* **1992**, *45*, 1746.
(152) Sin, N.; Kim, K. B.; Elofsson, M.; Meng, L.; Auth, H.; Kwok, B. H.; Crews, C. M. *Bioorg. Med. Chem. Lett.* **1999**, *9*, 2283.
(153) Meng, L.; Kwok, B. H.; Sin, N.; Crews, C. M. *Cancer Res* **1999**, *59*, 2798.
(154) Kim, K. B.; Myung, J.; Sin, N.; Crews, C. M. *Bioorg. Med. Chem. Lett.* **1999**, *9*, 3335.
(155) Meng, L.; Mohan, R.; Kwok, B. H.; Elofsson, M.; Sin, N.; Crews, C. M. *Proc. Natl. Acad. Sci. U.S.A.* **1999**, *96*, 10403.
(156) Groll, M.; Koguchi, Y.; Huber, R.; Kohno, J. *J. Mol. Biol.* **2001**, *311*, 543.
(157) Baldwin, J. *Ciba Found. Symp.* **1978**, 85.
(158) Koguchi, Y.; Kohno, J.; Suzuki, S.; Nishio, M.; Takahashi, K.; Ohnuki, T.; Komatsubara, S. *J. Antibiot. (Tokyo)* **1999**, *52*, 1069.
(159) Koguchi, Y.; Nishio, M.; Suzuki, S.; Takahashi, K.; Ohnuki, T.; Komatsubara, S. *J. Antibiot. (Tokyo)* **2000**, *53*, 967.
(160) Koguchi, Y.; Kohno, J.; Suzuki, S.; Nishio, M.; Takahashi, K.; Ohnuki, T.; Komatsubara, S. *J. Antibiot. (Tokyo)* **2000**, *53*, 63.
(161) Omura, S.; Fujimoto, T.; Otoguro, K.; Matsuzaki, K.; Moriguchi, R.; Tanaka, H.; Sasaki, Y. *J. Antibiot. (Tokyo)* **1991**, *44*, 113.
(162) Omura, S.; Matsuzaki, K.; Fujimoto, T.; Kosuge, K.; Furuya, T.; Fujita, S.; Nakagawa, A. *J. Antibiot. (Tokyo)* **1991**, *44*, 117.
(163) Takahashi, S.; Uchida, K.; Nakagawa, A.; Miyake, Y.; Kainosho, M.; Matsuzaki, K.; Omura, S. *J. Antibiot. (Tokyo)* **1995**, *48*, 1015.
(164) Fenteany, G.; Standaert, R. F.; Reichard, G. A.; Corey, E. J.; Schreiber, S. L. *Proc. Natl. Acad. Sci. U.S.A.* **1994**, *91*, 3358.
(165) Katagiri, M.; Hayashi, M.; Matsuzaki, K.; Tanaka, H.; Omura, S. *J. Antibiot. (Tokyo)* **1995**, *48*, 344.
(166) Fenteany, G.; Standaert, R. F.; Lane, W. S.; Choi, S.; Corey, E. J.; Schreiber, S. L. *Science* **1995**, *268*, 726.
(167) Imajoh-Ohmi, S.; Kawaguchi, T.; Sugiyama, S.; Tanaka, K.; Omura, S.; Kikuchi, H. *Biochem. Biophys. Res. Commun.* **1995**, *217*, 1070.
(168) Craiu, A.; Gaczynska, M.; Akopian, T.; Gramm, C. F.; Fenteany, G.; Goldberg, A. L.; Rock, K. L. *J. Biol. Chem.* **1997**, *272*, 13437.
(169) Dick, L. R.; Cruikshank, A. A.; Grenier, L.; Melandri, F. D.; Nunes, S. L.; Stein, R. L. *J. Biol. Chem.* **1996**, *271*, 7273.
(170) Corey, E. J.; Li, W. D. *Chem. Pharm. Bull. (Tokyo)* **1999**, *47*, 1.
(171) Bürgi, H.; Dunitz, J.; Shefter, E. *J. Am. Chem. Soc.* **1973**, *95*, 5065.

(172) Feling, R. H.; Buchanan, G. O.; Mincer, T. J.; Kauffman, C. A.; Jensen, P. R.; Fenical, W. *Angew. Chem., Int. Ed.* **2003**, *42*, 355.
(173) Maldonado, L. A.; Fenical, W.; Jensen, P. R.; Kauffman, C. A.; Mincer, T. J.; Ward, A. C.; Bull, A. T.; Goodfellow, M. *Int. J. Syst. Evol. Microbiol.* **2005**, *55*, 1759.
(174) Chauhan, D.; Catley, L.; Li, G.; Podar, K.; Hideshima, T.; Velankar, M.; Mitsiades, C.; Mitsiades, N.; Yasui, H.; Letai, A.; Ovaa, H.; Berkers, C.; Nicholson, B.; Chao, T. H.; Neuteboom, S. T.; Richardson, P.; Palladino, M. A.; Anderson, K. C. *Cancer Cell* **2005**, *8*, 407.
(175) Macherla, V. R.; Mitchell, S. S.; Manam, R. R.; Reed, K. A.; Chao, T. H.; Nicholson, B.; Deyanat-Yazdi, G.; Mai, B.; Jensen, P. R.; Fenical, W. F.; Neuteboom, S. T.; Lam, K. S.; Palladino, M. A.; Potts, B. C. *J. Med. Chem.* **2005**, *48*, 3684.
(176) Williams, P. G.; Buchanan, G. O.; Feling, R. H.; Kauffman, C. A.; Jensen, P. R.; Fenical, W. *J. Org. Chem.* **2005**, *70*, 6196.
(177) Asai, A.; Hasegawa, A.; Ochiai, K.; Yamashita, Y.; Mizukami, T. *J. Antibiot. (Tokyo)* **2000**, *53*, 81.
(178) Armstrong, A.; Scutt, J. N. *Org. Lett.* **2003**, *5*, 2331.
(179) Larionov, O. V.; de Meijere, A. *Org. Lett.* **2004**, *6*, 2153.
(180) Armstrong, A.; Scutt, J. N. *Chem. Commun. (Cambridge, U.K.)* **2004**, 510.
(181) Asai, A.; Tsujita, T.; Sharma, S. V.; Yamashita, Y.; Akinaga, S.; Funakoshi, M.; Kobayashi, H.; Mizukami, T. *Biochem. Pharmacol.* **2004**, *67*, 227.
(182) Toes, R. E.; Nussbaum, A. K.; Degermann, S.; Schirle, M.; Emmerich, N. P.; Kraft, M.; Laplace, C.; Zwinderman, A.; Dick, T. P.; Muller, J.; Schonfisch, B.; Schmid, C.; Fehling, H. J.; Stevanovic, S.; Rammensee, H. G.; Schild, H. *J. Exp. Med.* **2001**, *194*, 1.
(183) Shinohara, K.; Tomioka, M.; Nakano, H.; Tone, S.; Ito, H.; Kawashima, S. *Biochem. J.* **1996**, *317*, 385.
(184) Hideshima, T.; Richardson, P.; Chauhan, D.; Palombella, V. J.; Elliott, P. J.; Adams, J.; Anderson, K. C. *Cancer Res.* **2001**, *61*, 3071.
(185) Koguchi, Y.; Kohno, J.; Nishio, M.; Takahashi, K.; Okuda, T.; Ohnuki, T.; Komatsubara, S. *J. Antibiot. (Tokyo)* **2000**, *53*, 105.
(186) Kohno, J.; Koguchi, Y.; Nishio, M.; Nakao, K.; Kuroda, M.; Shimizu, R.; Ohnuki, T.; Komatsubara, S. *J. Org. Chem.* **2000**, *65*, 990.
(187) Lin, S.; Danishefsky, S. J. *Angew. Chem., Int. Ed.* **2001**, *40*, 1967.
(188) Kaiser, M.; Groll, M.; Renner, C.; Huber, R.; Moroder, L. *Angew. Chem., Int. Ed.* **2002**, *41*, 780.
(189) Lin, S.; Danishefsky, S. J. *Angew. Chem., Int. Ed.* **2002**, *41*, 512.
(190) Inoue, M.; Sakazaki, H.; Furuyama, H.; Hirama, M. *Angew. Chem., Int. Ed.* **2003**, *42*, 2654.
(191) Kaiser, M.; Groll, M.; Siciliano, C.; Assfalg-Machleidt, I.; Weyher, E.; Kohno, J.; Milbradt, A. G.; Renner, C.; Huber, R.; Moroder, L. *ChemBioChem* **2004**, *5*, 1256.
(192) Albrecht, B. K.; Williams, R. M. *Proc. Natl. Acad. Sci. U.S.A.* **2004**, *101*, 11949.
(193) Kaiser, M.; Milbradt, A.; Siciliano, C.; Assfalg-Machleidt, I.; Machleidt, W.; Groll, M.; Renner, C.; Moroder, L. *Chem. Biodiversity* **2004**, *1*, 161.
(194) Janetka, J. W.; Satyshur, K. A.; Rich, D. H. *Acta Crystallogr., C* **1996**, *52* (Part 12), 3112.
(195) Janetka, J.; Raman, P.; Satyshur, K.; Flentke, G.; Rich, D. *J. Am. Chem. Soc.* **1997**, *119*, 441.
(196) Muller, G.; Giera, H. *J. Comput. Aided Mol. Des.* **1998**, *12*, 1.
(197) Groll, M.; Götz, M.; Kaiser, M.; Weyher, E.; Moroder, L. *Chem. Biol.* **2006**, *13* (6), 607.
(198) Vigneron, N.; Stroobant, V.; Chapiro, J.; Ooms, A.; Degiovanni, G.; Morel, S.; van der Bruggen, P.; Boon, T.; Van den Eynde, B. J. *Science* **2004**, *304*, 587.
(199) Lin, K. I.; Baraban, J. M.; Ratan, R. R. *Cell Death Differ.* **1998**, *5*, 577.
(200) Ostrowska, H.; Wojcik, C.; Omura, S.; Worowski, K. *Biochem. Biophys. Res. Commun.* **1997**, *234*, 729.
(201) Sherwood, S. W.; Kung, A. L.; Roitelman, J.; Simoni, R. D.; Schimke, R. T. *Proc. Natl. Acad. Sci. U.S.A.* **1993**, *90*, 3353.
(202) Wojcik, C.; Schroeter, D.; Stoehr, M.; Wilk, S.; Paweletz, N. *Eur. J. Cell Biol.* **1996**, *70*, 172.
(203) Josefsberg, L. B.; Galiani, D.; Dantes, A.; Amsterdam, A.; Dekel, N. *Biol. Reprod.* **2000**, *62*, 1270.
(204) Chmelikova, E.; Sedmikova, M.; Rajmon, R.; Petr, J.; Svestkova, D.; Jilek, F. *Zygote* **2004**, *12*, 157.
(205) Tan, X.; Peng, A.; Wang, Y.; Tang, Z. *Sci. China, Ser. C: Life Sci.* **2005**, *48*, 287.
(206) Marangos, P.; Carroll, J. *Dev. Biol.* **2004**, *272*, 26.
(207) Drexler, H. C. *Apoptosis* **1998**, *3*, 1.
(208) Orlowski, R. Z. *Cell Death Differ.* **1999**, *6*, 303.
(209) Grimm, L. M.; Goldberg, A. L.; Poirier, G. G.; Schwartz, L. M.; Osborne, B. A. *EMBO J.* **1996**, *15*, 3837.
(210) Sadoul, R.; Fernandez, P. A.; Quiquerez, A. L.; Martinou, I.; Maki, M.; Schroter, M.; Becherer, J. D.; Irmler, M.; Tschopp, J.; Martinou, J. C. *EMBO J.* **1996**, *15*, 3845.
(211) Drexler, H. C. *Proc. Natl. Acad. Sci. U.S.A.* **1997**, *94*, 855.
(212) Lopes, U. G.; Erhardt, P.; Yao, R.; Cooper, G. M. *J. Biol. Chem.* **1997**, *272*, 12893.
(213) An, W. G.; Chuman, Y.; Fojo, T.; Blagosklonny, M. V. *Exp. Cell Res.* **1998**, *244*, 54.
(214) Drexler, H. C.; Risau, W.; Konerding, M. A. *FASEB J.* **2000**, *14*, 65.
(215) Meriin, A. B.; Gabai, V. L.; Yaglom, J.; Shifrin, V. I.; Sherman, M. Y. *J. Biol. Chem.* **1998**, *273*, 6373.
(216) Bush, K. T.; Goldberg, A. L.; Nigam, S. K. *J. Biol. Chem.* **1997**, *272*, 9086.
(217) Lee, D. H.; Goldberg, A. L. *Mol. Cell. Biol.* **1998**, *18*, 30.
(218) Kinyamu, H. K.; Chen, J.; Archer, T. K. *J. Mol. Endocrinol.* **2005**, *34*, 281.
(219) Ferdous, A.; Gonzalez, F.; Sun, L.; Kodadek, T.; Johnston, S. A. *Mol. Cell* **2001**, *7*, 981.
(220) Gillette, T. G.; Gonzalez, F.; Delahodde, A.; Johnston, S. A.; Kodadek, T. *Proc. Natl. Acad. Sci. U.S.A.* **2004**, *101*, 5904.
(221) Muratani, M.; Tansey, W. P. *Nat. Rev. Mol. Cell Biol.* **2003**, *4*, 192.
(222) Russell, S. J.; Reed, S. H.; Huang, W.; Friedberg, E. C.; Johnston, S. A. *Mol. Cell* **1999**, *3*, 687.
(223) Lee, D.; Ezhkova, E.; Li, B.; Pattenden, S. G.; Tansey, W. P.; Workman, J. L. *Cell* **2005**, *123*, 423.
(224) Rock, K. L.; Goldberg, A. L. *Annu. Rev. Immunol.* **1999**, *17*, 739.
(225) Groettrup, M.; Schmidtke, G. *Drug Discovery Today* **1999**, *4*, 63.
(226) Ciechanover, A.; Schwartz, A. L. *Proc. Natl. Acad. Sci. U.S.A.* **1998**, *95*, 2727.
(227) Colmegna, I.; Sainz, B., Jr.; Garry, R. F.; Espinoza, L. R. *J. Rheumatol.* **2005**, *32*, 1192.
(228) Doherty, F. J.; Dawson, S.; Mayer, R. J. *Essays Biochem.* **2002**, *38*, 51.
(229) Richardson, P. G.; Sonneveld, P.; Schuster, M. W.; Irwin, D.; Stadtmauer, E. A.; Facon, T.; Harousseau, J. L.; Ben-Yehuda, D.; Lonial, S.; Goldschmidt, H.; Reece, D.; San-Miguel, J. F.; Blade, J.; Boccadoro, M.; Cavenagh, J.; Dalton, W. S.; Boral, A. L.; Esseltine, D. L.; Porter, J. B.; Schenkein, D.; Anderson, K. C. *N. Engl. J. Med.* **2005**, *352*, 2487.
(230) Mitsiades, C. S.; Mitsiades, N.; Hideshima, T.; Richardson, P. G.; Anderson, K. C. *Essays Biochem.* **2005**, *41*, 205.
(231) Whang, P. G.; Gamradt, S. C.; Gates, J. J.; Lieberman, J. R. *Prostate Cancer Prostatic Dis.* **2005**, *8*, 327.
(232) Perez-Galan, P.; Roue, G.; Villamor, N.; Montserrat, E.; Campo, E.; Colomer, D. *Blood* **2006**, *107*, 257.
(233) Schenkein, D. P. *Clin. Lung Cancer* **2005**, *7* (Suppl. 2), S49.
(234) Hideshima, T.; Chauhan, D.; Ishitsuka, K.; Yasui, H.; Raje, N.; Kumar, S.; Podar, K.; Mitsiades, C.; Hideshima, H.; Bonham, L.; Munshi, N. C.; Richardson, P. G.; Singer, J. W.; Anderson, K. C. *Oncogene* **2005**, *24*, 3121.
(235) Hougardy, B. M.; Maduro, J. H.; van der Zee, A. G.; Willemse, P. H.; de Jong, S.; de Vries, E. G. *Lancet Oncol.* **2005**, *6*, 589.
(236) Meiners, S.; Laule, M.; Rother, W.; Guenther, C.; Prauka, I.; Muschick, P.; Baumann, G.; Kloetzel, P. M.; Stangl, K. *Circulation* **2002**, *105*, 483.
(237) Wente, M. N.; Eibl, G.; Reber, H. A.; Friess, H.; Buchler, M. W.; Hines, O. J. *Oncol. Rep.* **2005**, *14*, 1635.
(238) Shirley, R. B.; Kaddour-Djebbar, I.; Patel, D. M.; Lakshmikanthan, V.; Lewis, R. W.; Kumar, M. V. *Neoplasia* **2005**, *7*, 1104.
(239) Daniel, K. G.; Kuhn, D. J.; Kazi, A.; Dou, Q. P. *Curr. Cancer Drug Targets* **2005**, *5*, 529.
(240) Watanabe, H.; Tanaka, Y.; Shimazu, Y.; Sugahara, F.; Kuwayama, M.; Hiramatsu, A.; Kiyotani, K.; Yoshida, T.; Sakaguchi, T. *Microbiol. Immunol.* **2005**, *49*, 835.
(241) Lindenthal, C.; Weich, N.; Chia, Y. S.; Heussler, V.; Klinkert, M. Q. *Parasitology* **2005**, *131*, 37.
(242) Schubert, U.; Ott, D. E.; Chertova, E. N.; Welker, R.; Tessmer, U.; Princiotta, M. F.; Bennink, J. R.; Krausslich, H. G.; Yewdell, J. W. *Proc. Natl. Acad. Sci. U.S.A.* **2000**, *97*, 13057.
(243) Ott, D. E.; Coren, L. V.; Sowder, R. C., 2nd; Adams, J.; Schubert, U. *J. Virol.* **2003**, *77*, 3384.
(244) Phillips, J. B.; Williams, A. J.; Adams, J.; Elliott, P. J.; Tortella, F. C. *Stroke* **2000**, *31*, 1686.
(245) Di Napoli, M.; McLaughlin, B. *Curr. Opin. Invest. Drugs* **2005**, *6*, 686.
(246) Di Napoli, M.; Papa, F. *Curr. Opin. Invest. Drugs* **2003**, *4*, 1333.
(247) Kalogeris, T. J.; Laroux, F. S.; Cockrell, A.; Ichikawa, H.; Okayama, N.; Phifer, T. J.; Alexander, J. S.; Grisham, M. B. *Am. J. Physiol.* **1999**, *276*, C856.
(248) Palombella, V. J.; Conner, E. M.; Fuseler, J. W.; Destree, A.; Davis, J. M.; Laroux, F. S.; Wolf, R. E.; Huang, J.; Brand, S.; Elliott, P. J.; Lazarus, D.; McCormack, T.; Parent, L.; Stein, R.; Adams, J.; Grisham, M. B. *Proc. Natl. Acad. Sci. U.S.A.* **1998**, *95*, 15671.
(249) Gaczynska, M.; Osmulski, P. A. *Methods Mol. Biol.* **2005**, *301*, 3.

(250) Darwin, K. H.; Ehrt, S.; Gutierrez-Ramos, J. C.; Weich, N.; Nathan, C. F. *Science* **2003**, *302*, 1963.

(251) Groll, M.; Huber, R. *Int. J. Biochem. Cell Biol.* **2003**, *35*, 606.

(252) Madden, D. R.; Gorga, J. C.; Strominger, J. L.; Wiley, D. C. *Cell* **1992**, *70*, 1035.

(253) Reed, K. A.; Maran, R. R.; Mitchell, S. S.; Xu, J.; Teisan, S.; Chao, T. H.; Deyanat-Yazdi, G.; Neuteboom, S. T.; Lam, K. S.; Potts, B. C. *J. Nat. Prod.*, published online Jan 23, http://dx.doi.org/10.1021/np0603471.

CR0502504